UCRL9504

UNIVERSITY OF CALIFORNIA

Ernest O. Lawrence

Radiation Laboratory

A THEORETICAL COMPARISON OF 4π FAST-NEUTRON SPECTROMETERS

DISCLAIMER

UCRL-9504
UC-37 Instruments
TID-4500 (16th Ed.)

UNIVERSITY OF CALIFORNIA

Lawrence Radiation Laboratory
Berkeley, California

Contract No. W-7405-eng-48

A THEORETICAL COMPARISON OF 4π FAST-NEUTRON SPECTROMETERS

Chul Mo Kim
(M.S. Thesis)

November 1960

Printed in USA. Price $1.75. Available from the
Office of Technical Services
U. S. Department of Commerce
Washington 25, D.C.

A THEORETICAL COMPARISON OF 4π FAST-NEUTRON SPECTROMETERS

Contents

Abstract 5

I. Introduction 6

A. Notations 7

B. Definitions 7

C. Basic Relations 8

II. Scintillation Counters

A. Plastic Scintillator 4π Neutron Spectrometer . . . 9

1. Efficiency 9

2. Energy Resolution 11

3. Useful Neutron-Energy Range 11

4. Directionality 13

5. Resolving Time 13

6. Gamma-Ray Discrimination 14

7. Remarks 15

B. He^4 Noble-Gas 4π Neutron Spectrometer . . . 16

1. Efficiency 16

2. Energy Resolution 16

3. Useful Neutron-Energy Range 17

4. Decay Time 17

5. Gamma-Ray Discrimination 17

6. Remarks 19

C. Li^6I(Eu) Inorganic-Scintillator 4π Neutron Spectrometer . 20

1. Efficiency 20

2. Energy Resolution 20

3. Useful Neutron-Energy Range 22

4. Decay Time 22

5. Gamma-Ray Discrimination 22

D. Double-Pulse Total-Absorption 4π Neutron Spectrometer 24

1. Efficiency 25

2. Energy Resolution 25
3. Useful Neutron Energy Range 26
4. Resolving Time 26
5. Gamma-Ray and Background Discrimination . . 26
E. Two Crystals with a Thin -dE/dx Anti-Crystal Between . 27
F. Two Crystals with a Ag Detector
to Select the Direction of Incident Neutrons . . . 29
III. Proportional Counters
A. $He^3(n,p)T$ Proportional Counter 4π Neutron Spectrometer . 31
1. Efficiency 31
2. Energy Resolution 33
3. Useful Neutron-Energy Range 34
4. Directionality 34
5. Decay Time 35
6. Gamma-Ray Discrimination 35
7. Remarks 35
B. Paraffin-Moderated BF_3 Proportional Counter . . 36
1. Efficiency 36
2. Energy Resolution 36
3. Useful Neutron-Energy Range 39
4. Directionality 39
5. Decay Time 39
6. Gamma-Ray Discrimination 39
C. Polyethylene-Lined Proportional Counter . . . 40
1. Efficiency 40
2. Energy Resolution 40
3. Useful Neutron-Energy Range 40
4. Decay Time 42
5. Gamma-Ray Response 42
IV. Photographic Methods
A. Nuclear Emulsion 43
1. Efficiency 43
2. Energy Resolution 46

3. Useful Neutron-Energy Range 46
4. Saturation Effects 49
5. Gamma-Ray and Background Discrimination . . 49
6. Remarks 50
B. Li^6-Loaded Nuclear Emulsion 51
1. Efficiency 51
2. Energy Resolution 51
3. Useful Neutron-Energy Range 51
4. Saturation Effects 51
5. Gamma-Ray and Background Discrimination . . 53
6. Remarks 53
V. Threshold Detectors as 4π Neutron Spectrometers . . 54
1. Efficiency 54
2. Energy Resolution 55
3. Saturation Effects 55
4. Gamma-Ray and Background Response . . 55
5. Remarks 55
VI. Semiconductor Fast-Neutron Detector 56
1. Efficiency 56
2. Energy Resolution 57
3. Useful Energy Range 57
4. Gamma-Ray and Background Discrimination . . 58
5. Time Response 58
6. Directionality 58
7. Remarks 58
VII. Conclusions 59
Acknowledgments 65
References 66

A THEORETICAL COMPARISON OF 4π FAST-NEUTRON SPECTROMETERS

Chul Mo Kim

Lawrence Radiation Laboratory
University of California
Berkeley, California

November 1960

ABSTRACT

The relative merits of various 4π fast-neutron spectrometers are compared on a theoretical basis. Such features as efficiency, energy resolution, useful energy range, directionality, time response, and gamma-ray and background sensitivity are considered, in order to select the most promising types of 4π fast-neutron spectrometer for further development.

I. INTRODUCTION

A number of fast-neutron spectrometers have been developed, most of which require collimation of the neutron source. In practice there are many situations where the direction of incident neutrons is essentially 4π, for examples, inside a reactor or in the stray radiation fields near reactors, accelerators and contaminated areas.

In principle, a collimator could be used to select only those neutrons traveling at a small solid angle, and a unidirectional neutron spectrometer could be placed at the ends of the collimator. This solution is not satisfactory for the following reasons: first, the presence of the collimator will distort the energy spectrum by scattering neutrons from its inner walls in a complicated manner; secondly, collimation of neutrons limits the counting rate to those neutrons which leave the source at a very small solid angle. This results in either long counting times or poor statistics. It should be mentioned that because of the high penetrating power of fast neutrons, collimation requires a relatively large and heavy collimator. This bulk is undesirable when a portable instrument is required.

To avoid this, development of 4π fast-neutron (0.01-20 Mev) spectrometers that count as large a fraction of the incident neutrons as possible with a modest energy resolution is desired.

In this thesis, such factors as efficiency, energy resolution, useful energy range, directionality, time response, and gamma-ray and background sensitivity are considered, with the object of selecting the most promising 4π fast-neutron spectrometer for further development. Estimated values are used to make comparisons where experimental data are not available.

It must be kept in mind that the numbers quoted are only intended to estimate relative performance and are subject to change with improved design and measurement techniques.

A. Notations

The following terms are supplied for convenience:

E = energy of neutron, or simply energy;
E_p = energy of recoil proton;
E_A = energy of recoil nucleus of mass number A;
B = bias energy;
H = pulse height;
A = mass number;
σ_H = total scattering cross section for neutrons on hydrogen atom;
σ_A = cross section for neutron on nucleus of mass number A;
N_H = number of H atoms per cm^3,
N_A = number of atoms of mass number A per cm^3;

B. Definitions

The following definitions apply throughout the thesis:

Efficiency $\eta(E) = \dfrac{\text{number of counts per sec}}{\text{total number of neutrons entering the counter per sec}}$.

Energy Resolution: $\delta(E) \equiv \dfrac{\Delta E}{E}$, (1)

where ΔE is the full width at half maximum at E.

Neutron flux ϕ: the sum of the path lengths of all neutrons in unit volume element in unit time, or, the number of neutrons that enter a a sphere of diametral plane area of 1 cm^2 per second.

Neutron energy flux in $\dfrac{\text{Mev}}{\text{cm}^2\,\text{sec}} \equiv E\phi$,

where ϕ is the flux as defined above.

Effective area A: defined as the diametral plane area for the case of a sphere. Thus, it follows that

$$A = \pi\left(\frac{3}{4}\right)^{2/3} \ell^{2/3} r^{4/3},$$

for the case of a cylinder of radius r and length ℓ.

Effective thickness d: defined as the ratio of the total sensitive volume to the effective area of the neutron detector. For example,

$$d = \frac{\frac{4}{3}\pi r^3}{\pi r^2} = 4/3\ r,$$

for a sphere of radius r, and

$$d = (4/3)^{2/3} \ell^{1/3} r^{2/3}$$

for a cylinder of radius r and length ℓ.

Decay time of ionization and proportional counter: time required for the signal voltage to reach half of its final value after the passage of an ionizing particle through the counter.

Decay time of scintillator: time required for the emission of the fraction 1-(1/e), or 63% of the photons after the arrival of an ionizing particle in the scintillator.

C. Basic Relations

Efficiency $\eta(E)$ is related by

$$\eta(E) = \frac{C(E)}{\phi(E)A} \quad , \tag{2}$$

where $C(E)$ is the number of counts per sec.

Maximum neutron flux ϕ_{max} that can be detected is related to maximum counting rate C_{max} by

$$\phi_{max}(E) = \frac{C(E)_{max}}{\eta(E)A} \quad . \tag{3}$$

The energy dependence of the counter efficiency should be compensated for by multiplying the measured spectrum by $1/\eta(E)$ to get the true energy spectrum.

II. SCINTILLATION COUNTERS

A. Plastic Scintillator 4π Neutron Spectrometer

Fast neutrons entering the plastic scintillator produce proton recoils which in turn produce flashes of light. A photomultiplier converts these flashes into electrical pulses whose magnitude is proportional to the intensity of the light, which is in turn approximately proportional to the total energy lost by the recoil protons in the plastic scintillator. These are pulse-height analyzed, differentiated, and subsequently unfolded to get a neutron-energy spectrum using Eq. (12) from Sec. IV-A, or simply recorded to get the neutron intensity. The disadvantage of the plastic scintillator, that it is an efficient detector of gamma rays as well as of neutrons, can be overcome by the newly discovered method of differentiating neutron and gamma-ray pulses through their different pulse shapes. This promises to produce a very simple 4π neutron spectrometer.

1. Efficiency

The efficiency $\eta(E)$ can be estimated by

$$\eta(E) \approx N_H \sigma_H(E) d\, f(ad)\left(1-\frac{B}{E}\right), \tag{4}$$

where $N_H \sigma_H(E)d$ is the probability of n-p scattering in plastic, and

$$f(ad) = \frac{1-\exp[-ad]}{ad} \tag{5}$$

is the factor for the attenuation of neutrons passing through the scintillator, where $a = N_H \sigma_H(E) + N_C \sigma_C(E)$ and $1-(B/E)$ is the ratio of the number of recoil protons with $E_p > B$ to the total number of recoil protons. Equation (4) is plotted in Fig. 1 for d = 1 in. using the plastic density of 1.06 g/cm^3. The actual efficiency of this spectrometer is smaller than the above estimated value, since not all the recoiled protons can be counted. Other minor effects on efficiency are the interaction of neutrons with carbon nuclei, edge effects, multiple n-p

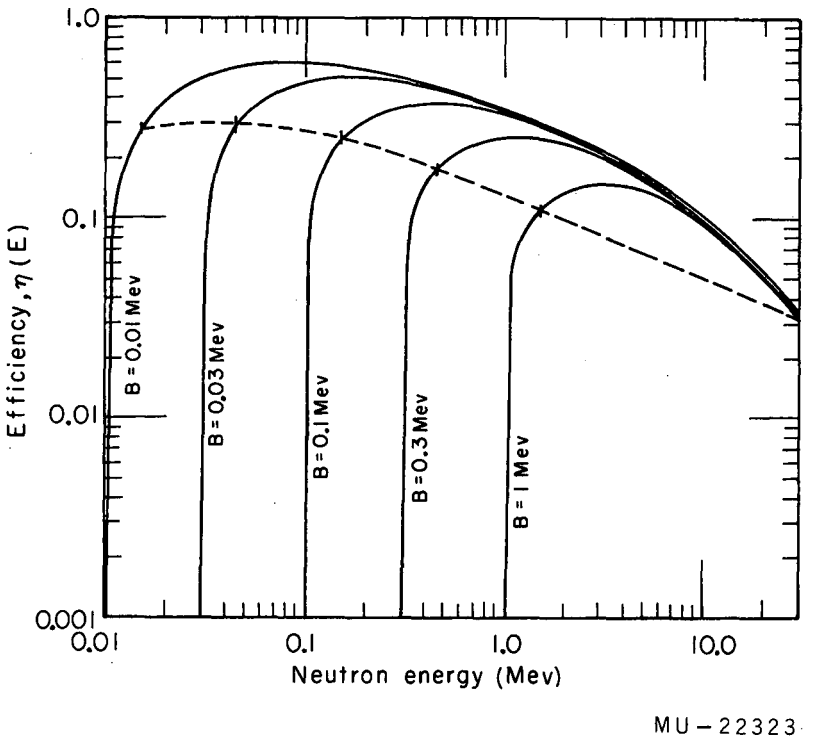

Fig. 1. Efficiency vs energy of plastic scintillator for d = 1 inch, and various values of B, plotted from Eq. (4) using a plastic density of 1.06 g/cm^2. Dotted line above (E_{min} = 1.5 B) shows the useful neutron energy range for values of biased-energy B setting.

scattering. These are discussed extensively by Swaltz and Owen[1] and Rybakov and Sidorov.[2]

2. Energy Resolution

The inherent limit in energy resolution of a plastic scintillator is due to statistical fluctuations of pulse height output, nonlinear response of plastic scintillators and effects of multiple scattering. Garlick and Wright found that the net result of the statistical fluctuations, in a stilbene scintillator and a photomultiplier combination, gives a distribution of the output pulse height H about a mean value $\bar{H}$,[3] reasonably well represented by the Gaussian function whose width varies approximately as $\bar{H}^{1/2}$ and is adjusted to be $\sigma = 0.05\,\bar{H}$ at $\bar{H}$ corresponding to 15 Mev proton energy, where σ is the standard deviation. These relations give

$$\frac{\Delta H}{\bar{H}} = \frac{0.334}{\bar{H}^{1/2}} \quad . \tag{6}$$

Swaltz and Owen[1] calculated and tabulated the nonlinear response of a scintillator for KB = 0.012 mg/cm^2 kev in Birk's semitheoretical formula for stilbene.[4] Assuming the above values for stilbene nearly true for plastic as well, the recoil proton energy resolution for a plastic scintillator is plotted in Fig. 2, using these values. Differentiation and subsequent unfolding of the recoil proton energy spectrum to get the neutron energy spectrum will introduce further broadening of energy resolution.

A plastic scintillator should be large enough so that a recoil proton of maximum energy can dissipate all its energy in the plastic, and small enough so that there is little effect on energy resolution due to the electron pulse height produced in the plastic scintillator.

3. Useful Neutron-Energy Range

Most of the plastic scintillators used have dimensions greater than 0.3 cm, the range of a 20-Mev proton. From Fig. 1 we see that the efficiency of the counter is large enough, and is a smoothly varying

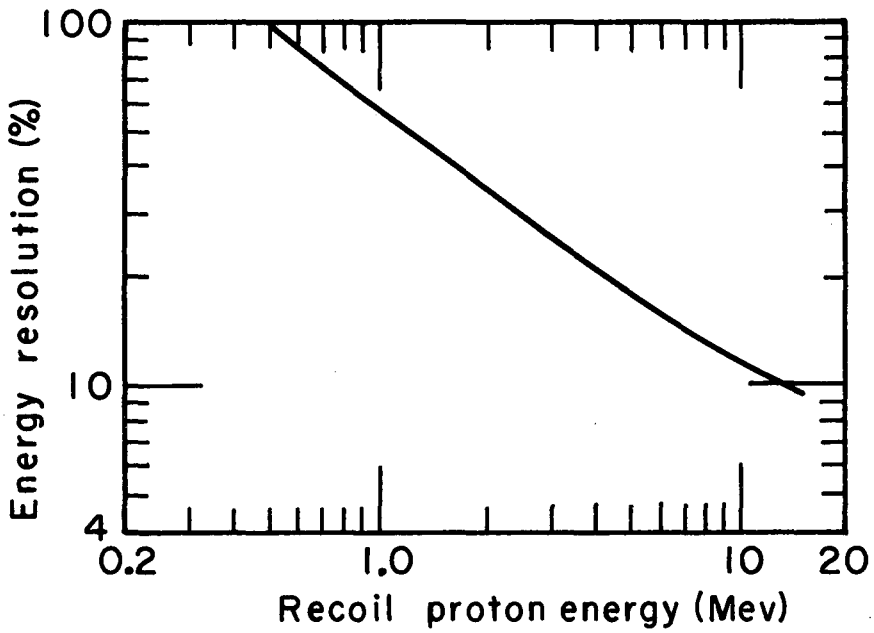

MU-22330

Fig. 2. Energy resolution vs proton energy, plotted from Eq. (6), using the nonlinear response of stilbene tabulated by Swaltz and Owen for KB = 0.012 mg/cm^2 in Birk's semitheoretical formula.

function of energy at 20 Mev. Thus it seems possible to use a plastic scintillator for 20-Mev neutrons.

The minimum neutron energy is determined by the bias energy B needed to bias-out background counts and get favorable counting rates with a reasonable energy resolution in the energy range we are interested in. Therefore, E should be greater than 1.5 B, since the slope of $\eta(E)$ vs E is very steep for $B < E < 1.5B$ (see Fig. 1). As shown in Fig. 2, a neutron energy smaller than 0.5 Mev is not measurable due to bad energy resolution. Muelhause has detected this energy as low as 0.1 Mev by employing a photomultiplier coincidence technique to suppress noise.[5]

4. Directionality

The total recoil energy that protons dissipate in the plastic scintillator is independent of the incident direction of the neutrons producing them. Thus, a plastic scintillator can be used as a 4π neutron spectrometer by using a scintillator of approximately spherical volume. This argument can be assumed to apply in general to the spectrometers discussed in the following sections and will not be restated unless directionality is explicitly discussed.

5. Resolving Time

Swank gives decay times of 3 mμ sec to 4.6 mμ sec for plastic scintillators.[6] Recovery time of the conventional electronic scaler is approx 1 mμ sec. Dead time of a pulse-height analyzer is 10 to 15 mμ sec plus 0.5 to 1 μ-sec per channel. A pulse-height analyzer generally has 100 to 200 channels. Thus average dead time of a conventional pulse-height analyzer is of the order of 50 μ sec. Since this time is much longer than the decay time of a scintillator, or the rise time of an electronic scaler, only the decay time will be mentioned in the spectrometers discussed hereafter. Using a 50 μ sec dead time, counting rates up to 200 counts/sec can be achieved with less than 1% dead-time loss. The above statement on the dead time of a pulse-height analyzer applies also to the spectrometers following that use a pulse-height analyzer.

6. Gamma-Ray Discrimination

The fundamental shortcoming of a plastic scintillator is that plastic scintillators are efficient detectors of gamma rays as well as of neutrons. Various methods have been devised to discriminate against gamma rays:

(a) Different pulse shape of protons and electrons:

The light pulses from protons have longer decay times than those from electrons. Owen[7] and Brooks[8] described experiments to discriminate against gamma rays using this method. Brooks[8] found that by using a 1-in. stilbene crystal, 2-Mev neutrons can be detected with 9.5% efficiency, and gamma rays of the same energy can be detected with an efficiency less than 0.007%.

(b) Size of plastics:[9, 10, 11]

Choose a size of plastic large enough for most recoil protons to dissipate their energy in the plastic scintillator, and small enough so that the electron pulse height produced is small when compared to the pulse height of the recoil protons.

(c) Coincidence and anti-coincidence method:[12]

If we use an inner spherical plastic viewed by a photomultiplier, and an outer concentric plastic spherical shell viewed by another photomultiplier, gamma rays can be discriminated by counting only those pulses from the central counter which are in anticoincidence with the pulses from the outer counters.

(d) Shielding the plastic:

Surround the plastic with the proper thickness of lead. The attenuation coefficient of gamma rays in lead is much larger than the macroscopic absorption cross section of neutrons, and increases as the energy of the gamma rays decreases, while the macroscopic absorption cross section of the neutron remains nearly constant within the fast-neutron energy range. Attenuation of a 0.1 Mev gamma-ray beam by a factor of 10 requires about 0.4 mm of lead, while this same

thickness of lead will almost fail to affect the fast-neutron beam. Thus, surrounding the scintillator with only about 1 mm of lead will attenuate most gamma rays of energy below 0.1-Mev, while fast-neutron beams are nearly unaffected.

7. Remarks

Using the gamma-ray discrimination methods suggested above, it seems possible to solve the fundamental disadvantage of a plastic scintillator as a neutron spectrometer. Then the plastic scintillator neutron spectrometer promises to be a very simple 4π neutron spectrometer with high efficiency and moderate energy resolution.

B. He^4 Noble-Gas 4π Neutron Spectrometer

Fast neutrons entering the He^4-filled scintillator produce He^4 recoils which in turn produce photons detected by a photomultiplier tube, the intensity of the light pulse being proportional to the energy of the α particle. The pulses are pulse-height analyzed and differentiated, then unfolded to get a neutron spectrum. Here the scintillating property of He^4 under the influence of ionizing radiation is used. The He^4 must be under pressure in order to limit recoils to a reasonable volume of the counter.

1. Efficiency

Efficiency $\eta(E)$ can be estimated by

$$\eta(E) \approx N_{He}\,\sigma_{He}(E)\,d\left(1-\frac{1.56B}{E}\right), \tag{7}$$

where $N_{He}\,\sigma_{He}\,d$ is the probability of scattering of a neutron in a He^4-filled counter, and

$$\int_B^{\alpha E} P(E)\,dE_A = \int_B^{\alpha E} \frac{dE_A}{\alpha E} = 1-\frac{B}{\alpha E} = 1-\frac{1.56B}{E} \tag{8}$$

is the ratio of recoil-He^4 atoms with $E_A > B$ to the total number of recoil, and $\alpha = 4A/(1+A)^2 = 0.64$ for He^4 nuclei. Equation (7) is plotted in Fig. 3 for the case of 5 atmospheres of He^4, with d = 10 cm. Northrop et al. observed maximum light output at a mixture of 10% Xe and 90% He^4.[13]

2. Energy Resolution

The energy resolution of a He^4 scintillator is determined by statistical fluctuations in the photomultiplier pulse-height output, wall and end effects, impurity of gas filling, and n-Xe collisions. Eggler and Huddleston constructed a gas scintillation spectrometer and obtained an energy resolution of 10% for 5-Mev alpha particles in a counter filled with 5 atmos of Argon.[14] Sayres and We obtained an

energy resolution of 4.8% for Po^{210} alpha particles (5.3 Mev), using xenon at 45 psi with quaterphenyl.[58] From this value we can estimate that the energy resolution of this counter will be better than 10% above 5 Mev, and more than 10% below 5 Mev. Diekirson shows that energy resolution improves as pressure in the counter increases.[15]

3. Useful Neutron-Energy Range

The range of 15-Mev α particles is about 1 m at atmospheric pressure of He^4. Thus a large high-pressure He^4 counter must be used to count 20-Mev neutrons. The addition of Xe improves light output as well as decreasing the range of recoil α particles.

E_{min} is determined by the bias energy B necessary to bias-out gamma rays. E_{min} of a He^4 counter should be greater than 2 B, since the slope of $\eta(E)$ vs E is very steep for $B < E < 2B$ (See Fig. 3). Due to low sensitivity of gamma rays in the He^4 scintillation counter, E_{min} is estimated to be about 0.1 Mev.

4. Decay Time

The decay time of a noble-gas scintillation counter is of the order of mμsec. Northrop and Noble found an inverse relationship between decay time and pressure for a gas chamber.[13]

5. Gamma-Ray Discrimination

One of the advantages of a He^4 scintillation counter is its strong discrimination against gamma rays due to its low density and low atomic number Z. Sayres and Wu obtained the pulse height of Po^{210} alpha particles (5.3 Mev) and radium gamma rays as 105 and 5 respectively for mixtures of 90% He and 10% Xe at 60 psi, using quaterphenyl.[58] Counter filling must be free of impurities for good background discrimination. Diekirson used a quartz window and eliminated the contaminent in the system due to the wave shifter.[15]

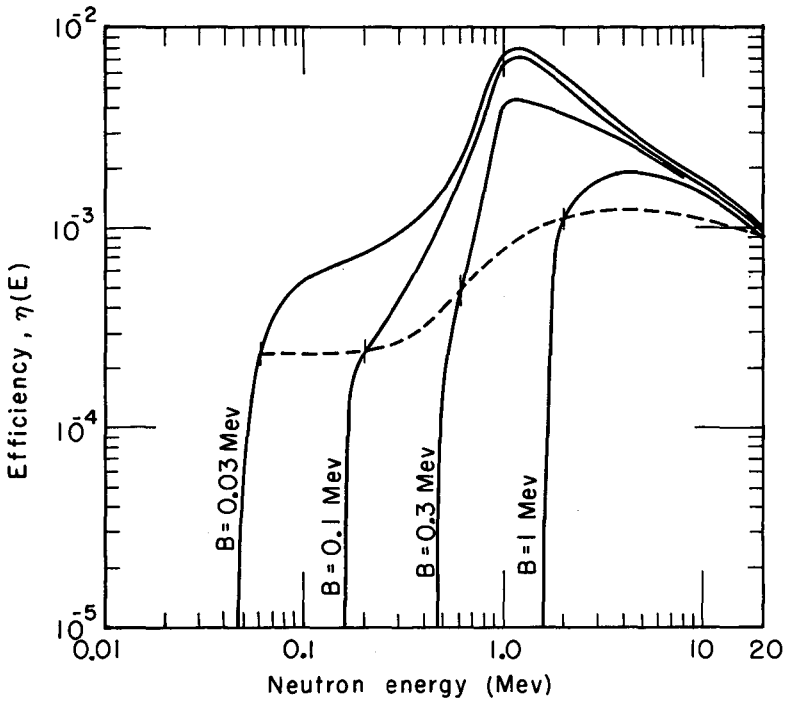

Fig. 3. Efficiency vs energy of He^4 scintillator counter, plotted from Eq. (7) for d = 10 cm and 5 atmospheres, for various values of B. The dotted line shows $E_{min} = 2B$.

6. Remarks

A He^4 scintillation counter has a fast decay time and a strong gamma discrimination. In addition, the pulse size of fission fragments is much greater than the background pulses from alpha particles, making this counter suitable for the study of the energy spectrum of fission fragments.

C. $Li^6I(Eu)$ Inorganic-Scintillator 4π Neutron Spectrometer

Fast neutrons entering a $Li^6I(Eu)$ inorganic scintillator react according to reaction $Li^6 + n \rightarrow He^4 + T + 4.78$ Mev. The resulting helium nucleus and triton dissipate their energy in the phosphor. This energy amounts to the sum of the incident neutron energy and the Q of 4.78 Mev. Eu atoms act as activation centers and re-emit energy in the form of a photon. The resulting pulses are pulse-height analyzed to give the neutron spectrum.

1. Efficiency

The efficiency of a $Li^6I(Eu)$ scintillator can be estimated from

$$\eta(E) \approx N_{Li^6} \sigma_{Li^6}(E)\, d\, f(ad), \qquad (9)$$

where $N_{Li^6} \sigma_{Li^6}(E)d$ is the probability of a $Li^6(n,d)T$ reaction in the $Li^6I(Eu)$ scintillator, and $f(ad) = (1-e^{-ad})/ad$ is the factor for the attenuation of neutron beams passing through the crystal where $A = N_{Li}\sigma_{Li}(E) + N_I \sigma_I(E)$, in which σ_{Li} and σ_I are the total cross sections of Li^6 and I respectively. Equation (9) is plotted in Fig. 4 for the various thicknesses of scintillator. The actual efficiency of the counter is smaller than the above value since not all the reaction products can be counted.

2. Energy Resolution

The energy resolution of this counter is proportional to $\Delta(E+Q)/E$. Thus, energy resolution gets poor as neutron energy decreases, due to the high Q (4.78 Mev) and the different scintillation efficiencies of an α and a T. Murray obtained a greatly improved energy resolution (30% for 3 Mev, 18% for 5.3 Mev and 7% for 14 Mev) by cooling the crystal to liquid nitrogen temperatures (Fig. 5).[17]

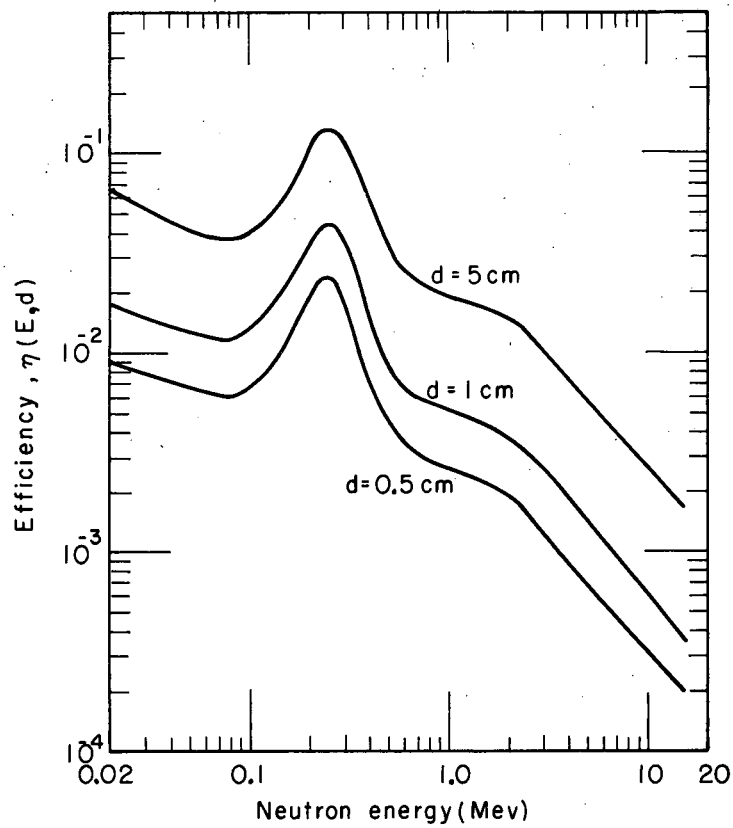

MU-22325

Fig. 4. Efficiency vs energy of $Li^6I(Eu)$ scintillator, plotted from Eq. (9) for various values of d.

3. Useful Neutron-Energy Range

E_{min} is about 1 Mev, since the distinction between a fast and a slow neutron pulse is not clear below 1 Mev. E_{max} is about 1 Mev, since pulses from competing reactions such as $Li^6(n, dn)He^4$, $Li^6(n, p)\ He^6$, and elastic scattering of neutrons on Li^6 set in at this and higher energies.

4. Decay Time

Decay time of about 1.2 μsec for a $Li^6I(Eu)$ inorganic scintillator is much longer than the decay time of organic or noble-gas scintillators.

5. Gamma-Ray Discrimination

Good discrimination against gamma rays of energies smaller than 4.78 Mev is possible due to high values of Q(4.78 Mev). Interference effects due to high-energy gamma rays can be eliminated by some of the methods suggested in Sec. I-A.

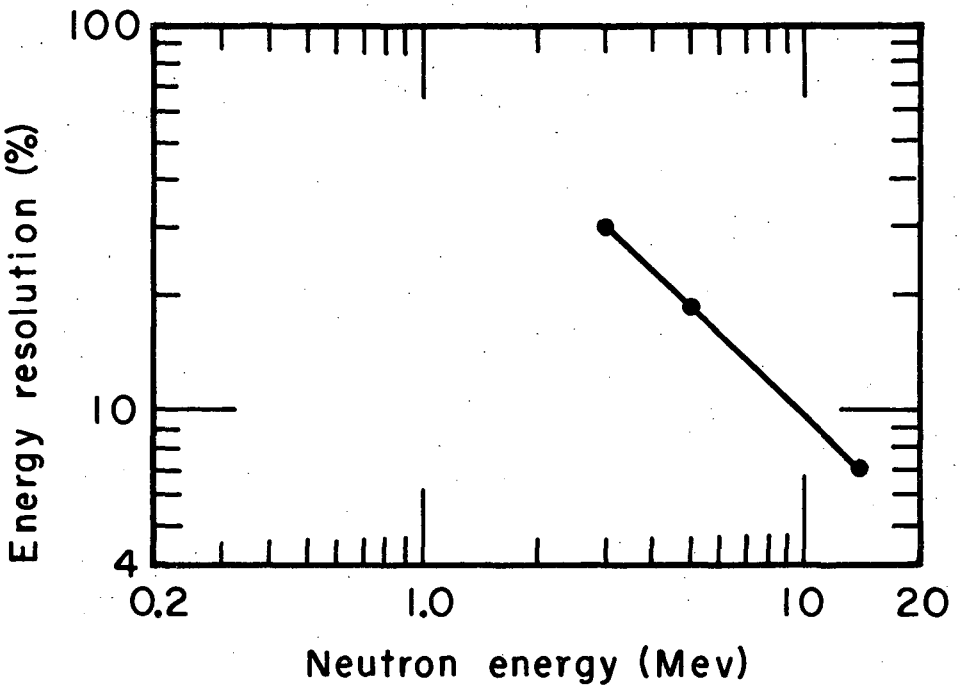

Fig. 5. Energy resolution vs energy of $Li^6I(Eu)$ scintillator. Points shown are values measured by Murray (see Ref. 17).

D. Double-Pulse Total-Absorption 4π

Neutron Spectrometer

Double-pulse total-absorption 4π neutron spectrometers are of two types. The first type is a cadmium- or boron-loaded organic liquid or solid scintillator viewed by photomultipliers, where fast neutrons are slowed down in the hydrogenous medium, and the slowed-down neutrons are absorbed in Cd^{113} or B^{10}, which have large absorption cross sections for low-energy neutrons. The resulting nuclei emit gamma rays or charged particles.

The second type is a plastic scintillator viewed by a photomultiplier surrounded by a BF_3 counter or a LiI(Eu) scintillator that identifies epithermal or thermal neutrons.

The same delayed-coincidence electronic technique is used in both types of spectrometer to identify those neutrons that lose most of their energy in the hydrogenous material, and the resulting pulses are pulse-height analyzed to get the neutron-energy spectrum. The delayed coincidence technique in both cases provides good gamma-ray discrimination.

The initial and delayed pulses are detected by the same photomultiplier in the first counter. Thus, the second type is relatively free of accidental coincidences compared to the first type. A large hydrogenous scintillator should be chosen if we want to use it for low-level counting not requiring high-energy resolution. Otherwise, the scintillator should be small enough to reduce the effects on energy resolution due to electron pulses produced in the scintillator, but large enough so that a recoil proton from a maximum-energy neutron can dissipate most of its energy in the scintillator.

Since both types are essentially the same detector, except for the differences mentioned above, we will discuss only the Cd-loaded organic-liquid scintillator.

1. Efficiency

The efficiency of a Cd-loaded organic-liquid scintillator is determined by the probability of neutrons not interacting in the scintillator, the probability of recoil neutrons escaping through the tank walls before being captured by Cd^{113}, and the fraction of capture-gamma pulses below the minimum counting bias. The mean distance of collision of a 20-Mev neutron in an organic liquid scintillator is about 40 cm. Thus, a scintillator with sufficiently large dimensions is necessary to count close to 100% for fast neutrons.

Reines et al. obtained an efficiency of 85% for a cylinder (30 in. high × 30 in. diam) with a Cd-to-H ratio of 0.00323.[18] This counter is suitable for low-level counting experiments due to its high efficiency.

2. Energy Resolution

The inherent limit in energy resolution of a Cd-loaded organic-liquid scintillator results from nonlinear response of the organic liquid scintillator, statistical fluctuations in the photomultiplier and scintillator, and occurrence of n-c collisions. Most important is the fact that neutron energy is measured from the sum of the recoil-proton energies collected within the finite gate width; that is, a neutron may lose all its energy in a single collision or from a large number of collisions. Andrew calculated pulse-height resolution as $\Delta H/H = 0.04E$ for this case,[19] where E is the energy of an incident neutron. This result gives better energy resolution as neutron energy decreases, while the other effects, such as the nonlinear response of pulse height vs proton energy, background, gamma effects, and photomultiplier noise, give better energy resolution at higher neutron energy. Thus, energy resolution is mainly affected by the latter effects at low energy and the former effect at higher energy. Since the energy resolution due to the latter effects is of the order of 10% at 1 Mev, these combined effects give an energy resolution of about 10% at 1 Mev and about 40% at 10 Mev.

3. Useful Neutron-Energy Range

E_{min} is determined by the bias energy necessary to bias-out gamma rays and noise. Muelhause gives E_{min} approx 1 Mev.[20] E_{max} is determined by the size of the counter.[20] Since the mean distance for the first collision with a proton for a 20-Mev neutron is about 40 cm, the counter dimension of a liquid scintillator should be sufficiently large to count a 20-Mev neutron.

4. Resolving Time

The decay time of an organic-liquid scintillation counter is a few mμsec, comparable to that of an organic-solid scintillator.

The average slowing down time to reach 0.1 kev, starting at 20 Mev, is about 0.3 μsec. An average delay time of approx 5 μsec and a gate width of approx 10 μsec is used.

5. Gamma-Ray and Background Discrimination

Since the pulse-height spectrum of 9.2-Mev gamma rays from Cd^{114*} is a continuum extending from zero to 9.2 Mev, much background can be easily eliminated by setting the bias energy at a suitable level. Also, the delayed coincidence used in this counter serves to discriminate gamma rays and background, and noise level can be reduced by cooling the organic-liquid scintillator.

Nicastro and Caswell suggested the B^{10}-loaded plastic scintillator for further development.[21] This would have the short resolving time and high cross section of B^{10} for slow neutrons.

E. Two Crystals with a Thin -dE/dx Anti-Crystal Between

This counter is constructed as shown in Fig. 6. Each of the two plastic scintillators is viewed by a separate photomultiplier, and a thin NaI(tl) crystal between plastic scintillators is viewed by a third photomultiplier.

The energy loss by a recoil proton while passing through the finite thickness of the NaI(tl) crystal is larger than that of an electron of the same energy owing to the low velocity of a proton as compared with an electron. Using this property, gamma rays and background can be discriminated by counting only those pulses formed by proton recoil that are in coincidence in all three crystals. The proton pulses are determined by the -dE/dx obtained in the NaI(tl) crystal, and by the total pulse height obtained in the three crystals at coincidence. But -dE/dx for recoil protons and electrons differs, depending upon the angle of incidence with respect to the NaI(tl) anti-crystal (Fig. 6). Thus, a 4π neutron spectrometer constructed by this method cannot adequately discriminate against gamma rays.

In view of a recent development in the successful discrimination of gamma rays using the different decay times of electron and proton pulses, this topic will not be pursued further here.

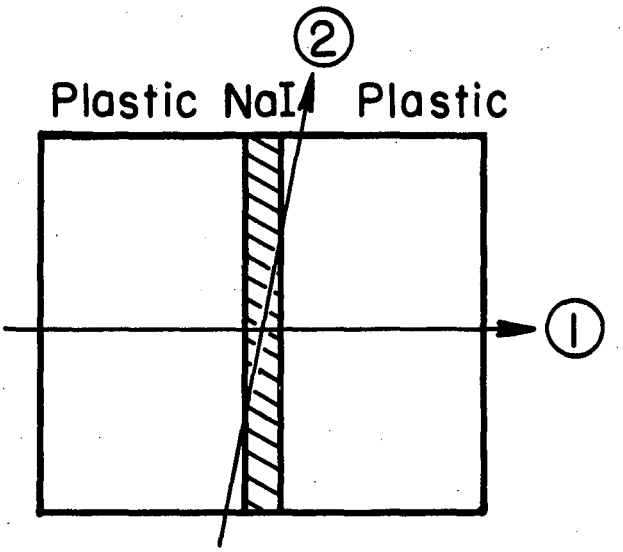

Fig. 6. Different -dE/dx for protons and electrons incident on NaI(Tl) anticrystals in different directions (1) and (2).

F. Two Crystals with a Ag Detector to Select the Direction of Incident Neutrons

Fast neutrons incident on an organic crystal, e.g., stilbene or plastic, produce proton recoils, and only those neutrons that lose most of their energy by head-on collisions with protons are counted, by placing the Ag-covered NaI(Tl) crystal normal to the direction of the incident neutrons (see Fig. 7). Slow neutrons captured by Ag, which has a large resonance cross section below 1 kev, produce gamma rays detectable in the NaI(Tl) crystal. The delayed-coincidence technique is used between proton-recoil pulses in the organic scintillator and gamma-ray pulses in NaI(Tl) to measure the neutron energy directly. Geometric alignment of two crystals can be used to determine the scattering angle of neutrons, but this method produces a low counting rate with a large statistical error. Higher counting rates are obtained by using the time-of-flight method that selects only coincidences due to the scattered neutrons of an energy less than a certain amount. The low-energy limit of scattered neutrons to be counted, together with the resolving time of the coincidence counter and the distance between the two crystals, is chosen to get the desired energy resolution and counting efficiency. This method requires a collimated neutron beam, and no satisfactory way of using this counter as a 4π neutron spectrometer has been devised.

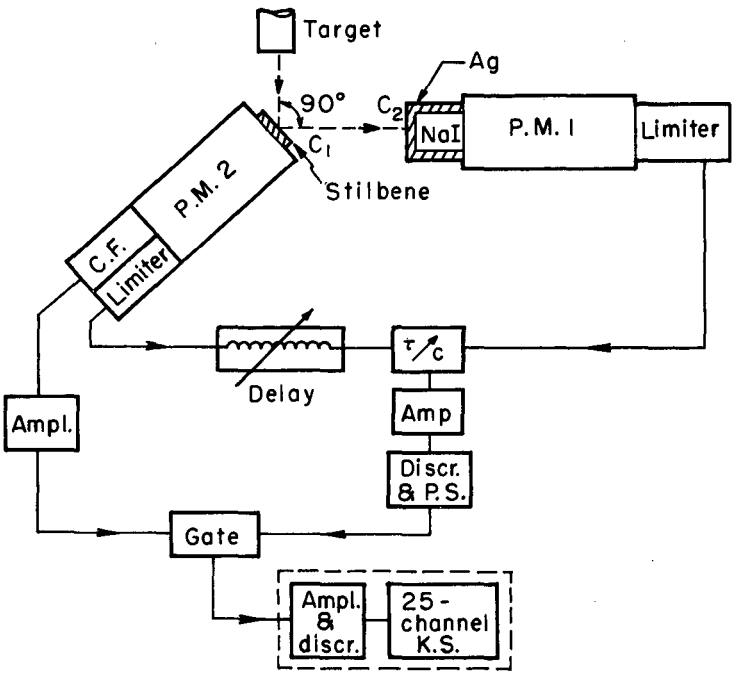

MU-22328

Fig. 7. Block diagram of spectrometer used by Beghian et al. employing two crystals with an Ag detector to select the direction of incident neutrons (see Ref. 22).

III. PROPORTIONAL COUNTERS

A. $He^3(n,p)T$ Proportional-Counter 4π Neutron Spectrometer

Neutrons incident on a He^3 proportional counter react according to the reaction $He^3 + n \rightarrow H + T + 0.77$ Mev. They may also just produce a He^3 recoil. Neutron energy is obtained from the combined energy that proton and tritium dissipate in the proportional counter. This is equal to the sum of 0.77 Mev plus incident neutron energy.

1. Efficiency

The efficiency of a $He^3(n,p)T$ proportional counter can be estimated from the reaction probability

$$N_{He^3}\, \sigma_{He^3}(E)\, d, \qquad (10)$$

where N_{He^3} is the number of He^3 atoms per unit sensitive volume of the counter, $\sigma_{He^3}(E)$ is the $He^3(n,p)T$ reaction cross section, and d is the effective thickness of the counter. Thus, high efficiency can be obtained by using high-pressure He^3 in the counter and as large a diameter for the proportional counter as permitted by the counter voltage. He^3 has become available in larger quantities, but technical difficulties that inhibit the obtaining of good energy resolution at high pressure must be overcome before high efficiency can be obtained.

The actual efficiency of the counter is smaller than the reaction probability mentioned above. Anticoincidence decreases system efficiency with increasing energy, because of increased wall effects. By using 5 cm as the effective size of the sensitive volume of the counter, and 5 atmos of He^3, we obtain a reaction probability of approx $6.24 \times 10^{-4}\, \sigma_{He^3}(E)$, as plotted in Fig. 8. At neutron energies of approx 1 Mev, the efficiency of the spectrometer used by Batchelor et al.[26] was 10^{-5}.

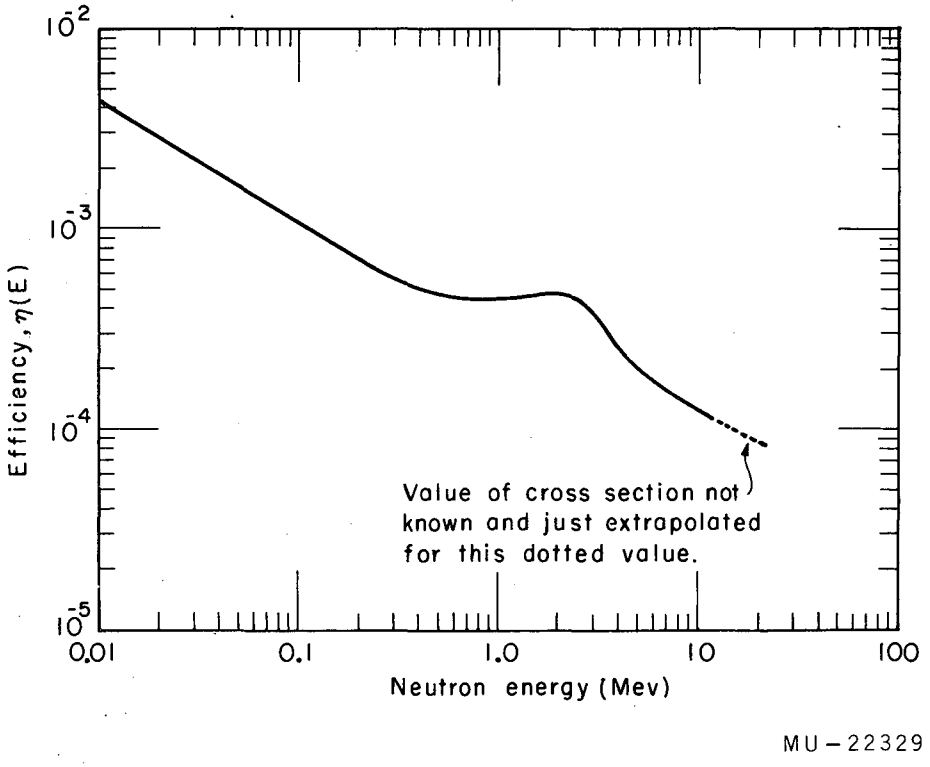

Fig. 8. Efficiency vs energy of $He^3(n.p)T$ proportional counter, plotted from Eq. (10) for d = 5 cm and 5 atmospheres of He^3. Actual efficiency is smaller than plotted reaction probability.

2. Energy Resolution

The following factors determine energy resolution.

(a) Statistics

According to West,[16] the inherent spread in pulse height for a proportional counter is $\Delta E/E = 2.36/m_0^{1/2}$, where m_0 is the mean number of ions initially released per incident particle in the counter. This gives a resolution of about 4 % at 0.1 Mev and 1.3 % at 1 Mev.

(b) Purity of gas filling

(1) Tritium content of He^3 should be as low as possible. 10^{-6} cc of tritium corresponds to approx 5×10^4 beta-disintegration pulses per sec, which pile up and produce additional spread in pulse height.

(2) The filling must be free from electron-capturing impurities such as O_2 and H_2O vapors. This is especially important at high energy.

(3) The filling must be free from polyatomic gases.

Since it is difficult to maintain the purity of the gas filling, it is advisable to use a permanent container.

(c) Wall and end effects

Wall effects can be reduced by keeping the proton and tritium ranges small compared to the size of the counter by introducing heavy gases such as Kr, A or Xe, increasing the pressure, using as large a counter as permitted by the counter voltage, and using an anticoincidence ring. This wall effect increases as the neutron energy increases. Detailed discussion of wall effects is given by Batchelor et al.[23] End effects can be eliminated by the method proposed by Cockcroft and Curran,[24] and Rossi and Staub.[25] Bothe and Stetter suggested that the use of very high pressures can be avoided by using a counter in which the sensitive volume is not defined by a solid wall.[59]

(d) Q value of 0.77 Mev

This Q value spoils energy resolution at low energies, since resolution is proportional to $\Delta(E+Q)/E$.

(e) Other effects

Other undesirable effects are such as variation of the anode diameter, variations in applied voltage, presence of dust particles on wire, and the position of ionization. Taking all these factors into account, it is reasonable to expect about 5% counter resolution, with He^3 completely free of tritium. The energy resolution of the counter used by Batchelor et al. was about 50% for E = 0.12 Mev and about 12% for E = 1 Mev.[23]

3. Useful Neutron Energy Range

There is a basic ambiguity in energy determination due to overlapping of the reaction $He^3(n,p)T$, Q = 0.77 Mev spectrum, and the recoil spectrum. The recoil spectrum extends from 0 to 3/4E, where E is the neutron energy producing He^3 recoil. The reaction spectrum produces a neutron peak at a total energy of Q + E for an incident neutron energy E.

If $E_{max} < Q4/3 = 1.025$ Mev, where E_{max} is the maximum neutron energy of the neutron spectrum, there is no ambiguity for the neutron-energy spectrum. If $E_{max} \gtrsim 1.025$ Mev, there is ambiguity for a continuous spectrum, but it can be analyzed in principle for neutron energies E between $3/4\ E_{max} - Q < E \leq E_{max}$, and for a neutron energy spectrum consisting of a distinct group.

E_{max} for a neutron energy spectrum may be raised by systematic removal of He^3 recoil spectra from a measured spectrum.

E_{min} is about 0.1 Mev, since for neutron energies below 0.1 Mev there is an overlapping of the 0.1-Mev neutron peak with the finite width of the thermal neutron peak.

4. Directionality

A cylindrical chamber with diameter equal to the height of the cylinder can be used as a roughly 4π neutron spectrometer, but a spherical chamber constructed by Salvini[26] is better than a cylindrical chamber for this purpose.

5. Decay Time

The decay time of a proportional counter is of the order of 1μsec.

6. Gamma-Ray Discrimination

This counter has an excellent gamma-ray discrimination for gamma-ray energies smaller than 0.77 Mev, since the neutrons which react with He^3 gain 0.77 Mev, but gamma rays do not. Using a counter with an anticoincidence ring, gamma rays and background can be discriminated by counting only those pulses from the central counter which are in anticoincidence with the pulses from outer counters.

7. Remarks

The advantages of an ion chamber relative to a proportional counter are that there are no impurity effects, and wall effects can be avoided by building a high-pressured large ion chamber such that the ranges of secondaries in the ion chamber are small relative to the counter dimension. The disadvantage of an ion chamber, the production of different pulse heights with respect to different chamber positions, can be avoided by using a grid plate.

B. Paraffin-Moderated BF_3 Proportional Counter

To measure the neutron energy spectrum, one measures the counting rate for a series of paraffin covers on a BF_3 counter, by using the detector efficiency $\Sigma i(E)$ from Figs. 9 and 10, one can obtain the absolute value of N(E) by doing a series of numerical integrations to get a value of C_i in agreement with the measured counting rate

$$C_i = \int N(E)\Sigma_i(E)dE, \qquad (11)$$

where C_i = counts/sec, Ni(E) = neutrons/cm^2 per sec Mev and $\Sigma_i(E)$ = counts/neutrons per cm^2. Subscript-i denotes a particular thickness of paraffin. From Fig. 10, we see that the counting rate of a paraffin-moderated BF_3 counter is constant, with energy within 10% when about 6 cm of paraffin is used inside the Cd cover. The Cd cover absorbs slow neutrons from the incident neutron flux, and 6 cm of paraffin provides just enough moderator to thermalize fast neutrons without excessive absorption. This counter, then, can be used for flux determination, and also to determine the average neutron energy by taking the ratio of the count rate from a polyethylene-lined proportional counter to the counting rate from a BF_3-filled proportional counter moderated with 6 cm of paraffin (see Sec. III-C).

1. Efficiency

Counting efficiency varies with the thickness of paraffin used, the sensitive area of the detector, and the energy of the neutrons (see Figs. 9 and 10). Efficiency is of the order of 10^{-2} and nearly constant within about 10% in the energy range of 10 kev to 10 Mev when 6 cm of paraffin cover is used.

2. Energy Resolution

The method described above to measure the energy spectrum by measuring the counting rates for a series of paraffin covers gives an energy resolution of the order of 50-100%, and is suitable where high energy resolution is not reuqired.

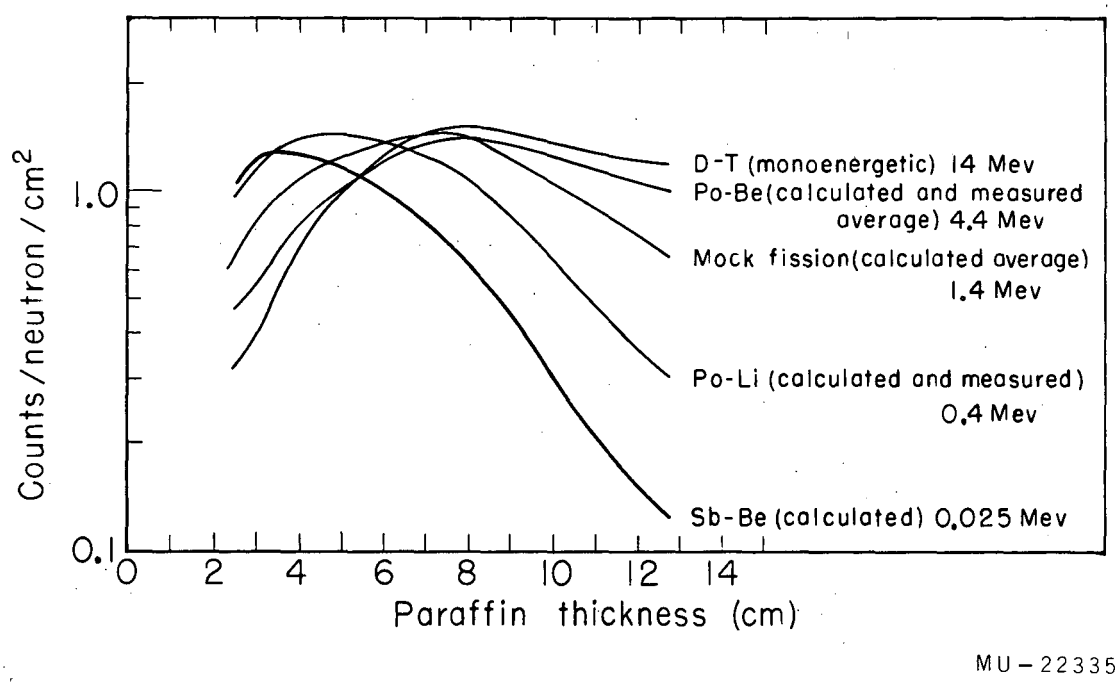

Fig. 9. BF_3 counting rate as a function of paraffin thickness for various neutron sources, corrected to an isotopic flux distribution. Entire assembly was covered with Cd (after Wallace et al see Ref. 29).

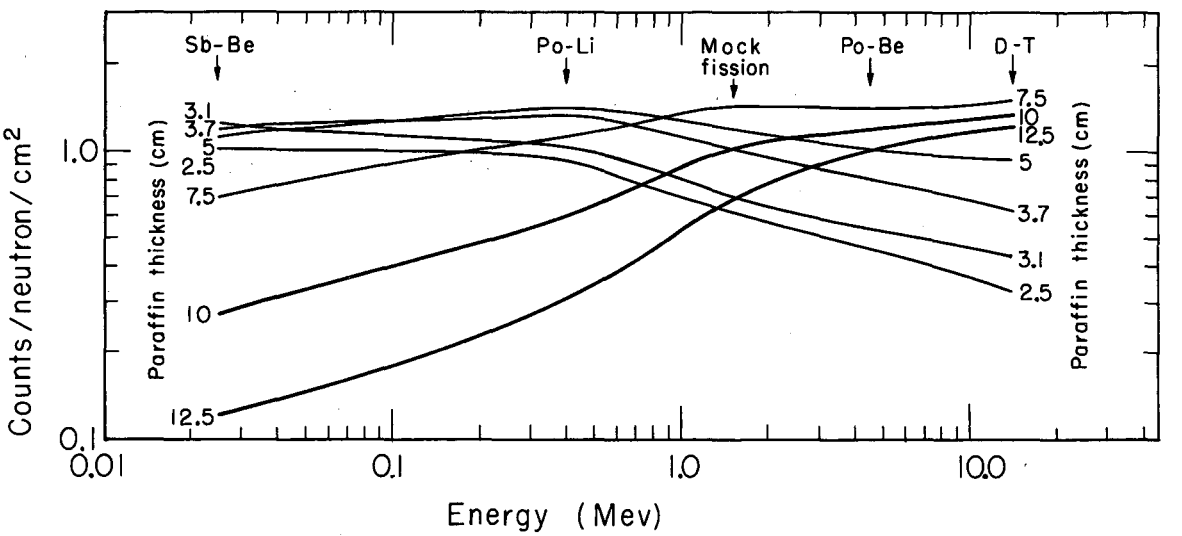

Fig. 10. Average efficiency of a BF_3 proportional counter as a function of neutron energy for various paraffin thickness, corrected to an isotopic flux distribution. Assemblies covered with Cd averaging over the 4π solid angle, have introduced error of up to 10% (after Wallace et al: see Ref. 29).

3. Useful Neutron-Energy Range

Hess et al. found that this counter is most useful in the energy range 10 kev to 10 Mev.[28]

4. Directionality

If the BF_3 proportional counter is constructed with diameter equal to height of sensitive volume, and surrounded with a uniform thickness of paraffin in all directions, it can be used as a 4π neutron counter.

5. Decay Time

The decay time of the proportionalcounter is approx 1 μ sec.

6. Gamma-Ray Discrimination

If one uses a suitable electronic bias, gamma rays can be easily discriminated due to the large value of $Q = 2.78$ Mev, from the reaction $B^{10}(n.d)Li^7$.

C. Polyethylene-Lined Proportional Counter

The polyethylene-lined proportional counter is constructed with a sheet of polyethylene bent into a cylinder and very lightly graphited with aquadag, the latter serving as the cathode of a proportional counter filled with A, CO_2 or methane.

Incident fast neutrons produce recoil protons from the polyethylene that dissipate their energy in the gas. The counting rate of the polyethylene-lined proportional counter is proportional to the energy flux and is used with an energy-in-sensitive detector to calculate the average neutron energy present in the field. This is done by taking the ratio of the counting rate in Mev/cm^2 per sec obtained from the polyethylene-lined proportional counter to the counting rate in n/cm^2/sec obtained from the energy-insensitive detector.

1. Efficiency

The efficiency calculated by Moyer[30] is reproduced in Fig. 11. As can be seen from the figure, the efficiency of the chamber is nearly proportional to the neutron energy from about 50 kev to 20 Mev for 1/8-in.-thick polyethylene. This counter actually records energy flux instead of the usual particle flux.

2. Energy Resolution

Energy resolution has no meaning for this counter, which measures energy flux instead of the usual particle flux. However, when used in conjunction with an energy-insensitive detector, for example a BF_3 proportional counter moderated with 6 cm of paraffin, the average neutron energy of a neutron spectrum can be measured.

3. Useful Neutron-Energy Range

By use of 1/8-in. thick polyethylene, the efficiency of the counter increases linearly with energy to 20 Mev. The gamma-ray background limits the minimum energy response to about 0.2 Mev.

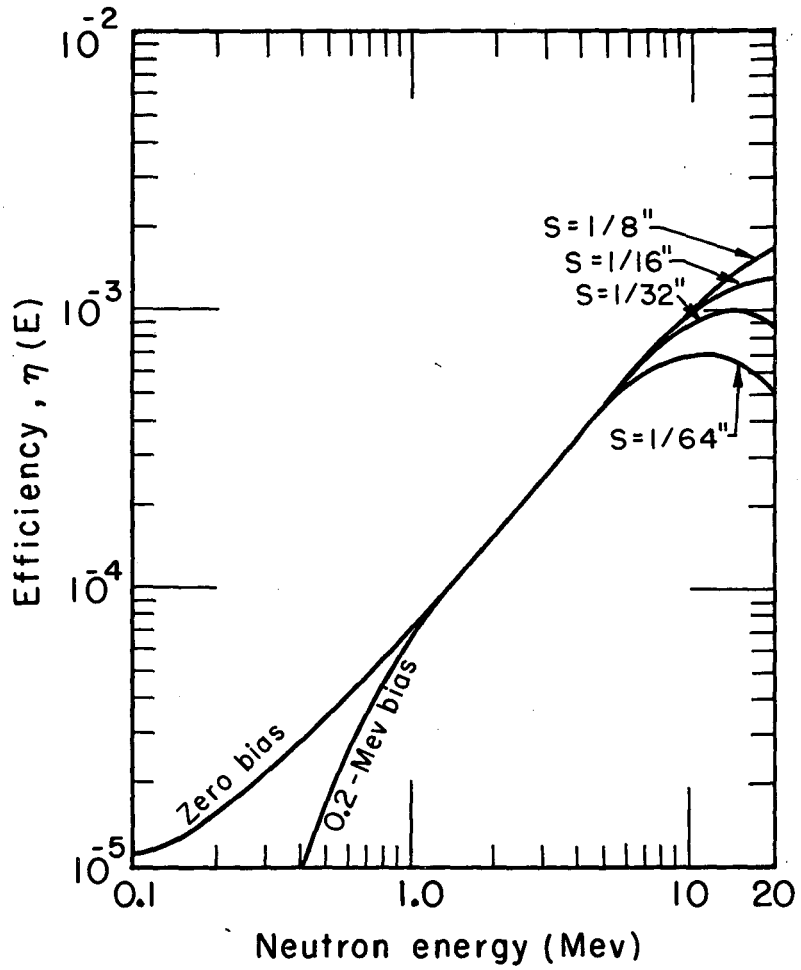

Fig. 11. Efficiency vs energy of a paraffin-moderated proportional counter for various paraffin wall thicknesses (after Moyer: see Rev. 30).

4. Decay Time

The decay time of a proportional counter is of the order of 1 μsec.

5. Gamma-Ray Response

Because of the low Z of the counter gases used in a polyethylene-lined proportional counter, electron pulses from photons are generally small enough to be biased-out by pulse-height rejection.

Thompson developed a scintillation counter which measures energy flux by coating the inner surface of a polyethylene spherical shell with a phosphor.[31] Scintillations produced by recoil protons are viewed with a photomultiplier tube through a suitable aperture. The energy flux can then be measured if the incident neutrons have velocities normal to the surface of the spherical shell. This counter has an acceptable counting rate at low flux levels, possesses good gamma discrimination, and is nondirectional.

IV. PHOTOGRAPHIC METHODS

A. Nuclear Emulsion

Neutrons traversing the emulsion produce proton tracks by recoil that can be measured by a semiautomatic method. The measured proton range distribution is corrected for recoil proton leakage, edge effects, emulsion shrinkage, cross section variation and other non-linearities. Leakage is corrected by using factor F, the fraction of proton recoils retained in a nuclear emulsion for an isotopic neutron source, and can be calculated from Figs. 12 and 13. The corrected proton energy range distribution dN_p/dE_p is inverted into the original neutron spectrum dN_n/dE through the relation

$$\frac{dN_n}{dE} = - \frac{1}{N_H d} \frac{E}{\sigma_H(E)} \frac{d}{dE_p} \frac{dN_p}{dE_p} , \qquad (12)$$

where $(d/dE_p)(dN_p/dE_p)$ is the slope of measured proton range distribution dN_p/dE_p and is negative. Various methods of measuring proton recoil tracks in nuclear emulsions are discussed by Reines,[32] Nereson and Reines,[33] Roberts,[34] and Evans.[35] In particular, Evans reports that anisotropic neutron spectra can be measured without the difficulties of recognizing and measuring accurately the nearly vertical tracks, and higher energies can be measured (without requiring a geometric correction) by exposing two nuclear plates at right angles to each other. In one plate, tracks at all azimuthal angles within ± 45 deg in the unprocessed emulsion from the plane of the emulsion are measured.

1. Efficiency

The efficiency of an emulsion is defined in terms of the average number of acceptable recoil proton tracks per incident neutron. It can be estimated from $N_H \sigma_H(E) d$, the scattering probability of a neutron on proton in the emulsion.

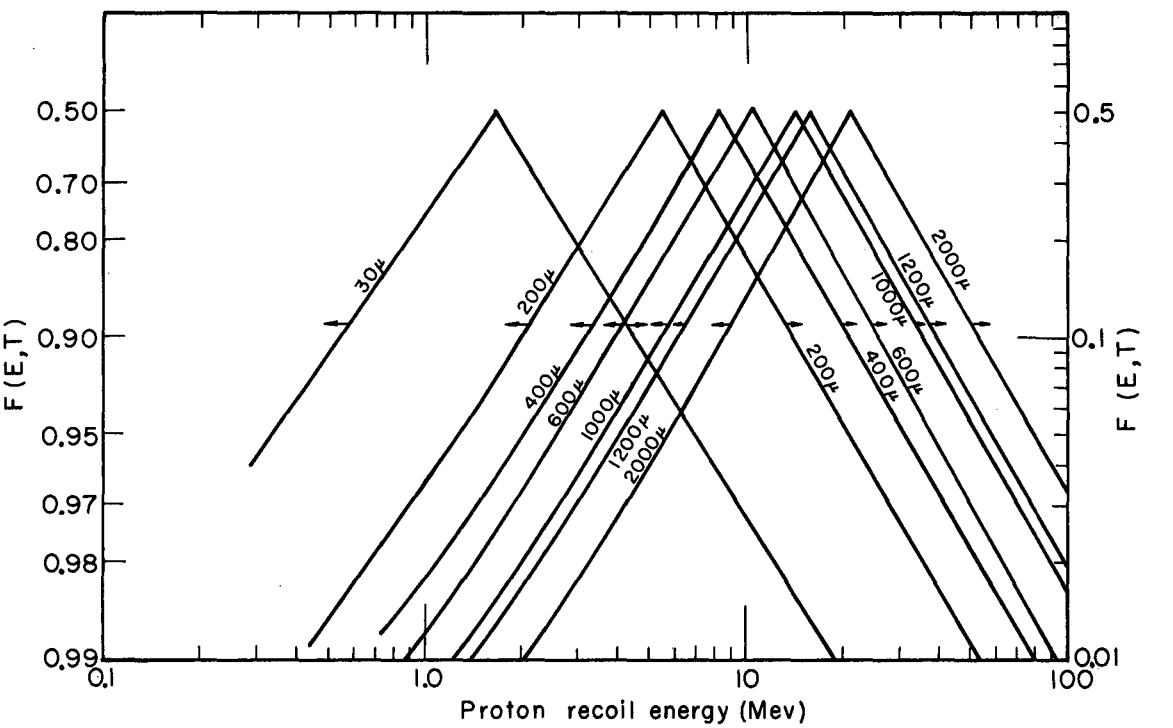

Fig. 12. Fraction $F(E,T)$ of proton recoils retained in nuclear emulsion vs proton recoil energy obtained by $F(E,T) = \frac{T-0.5\,R(E)}{T}$ for $R \leq T$ and $F(E,T) = \frac{T}{2R(E)}$, for $R \geq T$, where T = thickness of emulsion and $R(E)$ = range of proton recoils as a function of proton recoil energy (after D. Lehman of LRL, Berkeley).

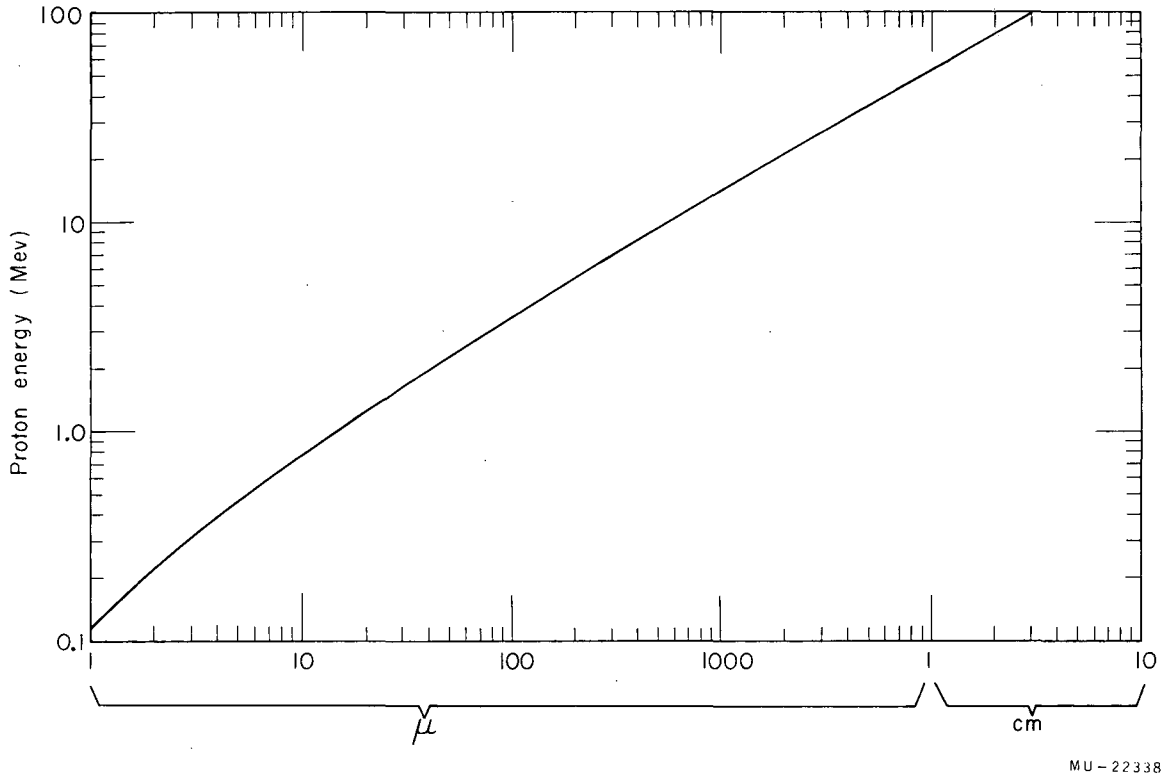

Fig. 13. Range vs proton energy in standard nuclear emulsion: 3.815 g/cm^3 at 60% relative humidity (after Barkas: see Ref. 38).

When emulsion 600 μ thick is used with a hydrogen content of approx 3.4×10^{22} atoms/cc, the value of $N_H \sigma_H(E)d$ is about $2\times10^{-3}\sigma_H(E)$, where $\sigma_H(E)$ is in barns. The value of $2\times10^{-3}\sigma_H(E)$ is plotted in Fig. 14.

2. Energy Resolution

Energy resolution depends upon the method used to count the proton tracks, the way these are used to calculate neutron spectra, and the following factors:

(a) Statistics of measurement error:

Uncertainty due to measurement error decreases as the number of measured tracks increases; usually about 3% per 10^3 proton tracks.

(b) Statistics of range straggling:

The energy resolution due to straggling decreases with increasing energy. According to Rotblat[36] it is about 1% for a proton energy greater than 3 Mev, and 20-100% below 0.5 Mev (see Fig. 15).

(c) Uncertainty due to the shrinkage factor:

This can be reduced well below 5% by careful handling of the emulaion, for example, by soaking it in glycerine or resin. The overall energy resolution can be made below 10% for $E > 3$ Mev when used with a collimated neutron beam. No differentiation is necessary for the case of a collimated neutron beam.

For isotopic neutron sources, differentiation of the proton recoil energy spectrum, taking into account the fraction of proton recoils retained in the emulsion, gives a resultant energy resolution much larger than 10%. Usually $\Delta E \approx 1$ Mev, and 50-100% energy resolution is obtained using 10^4 tracks. Evans reports energy resolutions of 32% at 0.827 Nev and 35% at 1.367 Mev were obtained using the method he has developed.[35]

3. Useful Neutron-Energy range

The range of 20-Mev protons in an emulsion is about 1.8 mm for an emulsion density of 3.815 g/cm^3 and relative humidity of 60% (see

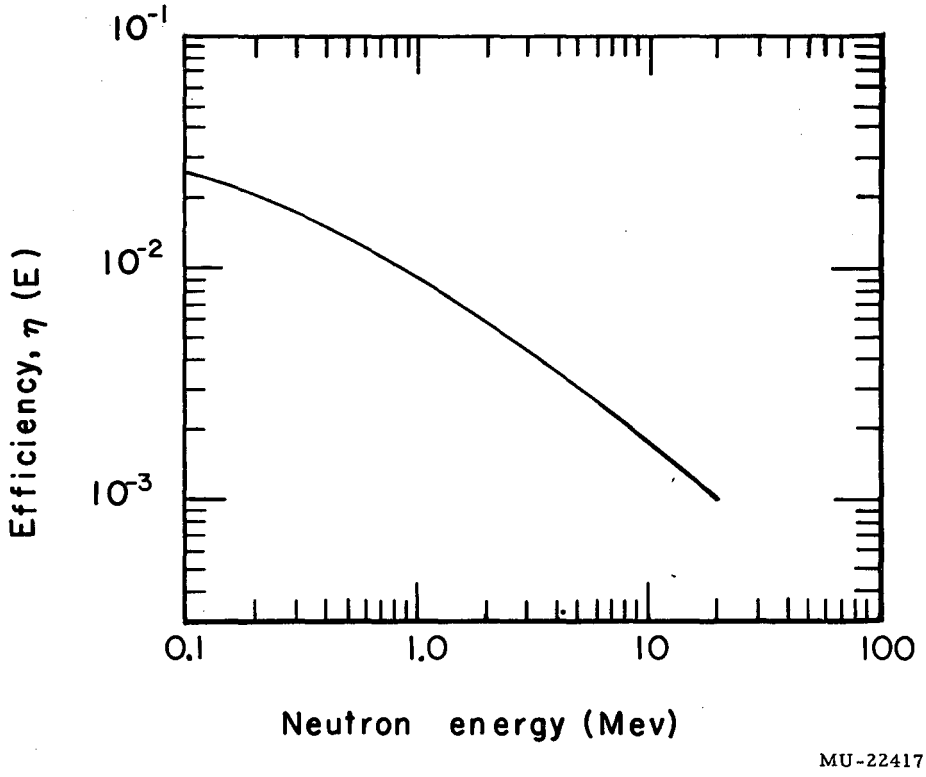

Fig. 14. Efficiency vs energy of nuclear emulsion, plotted from reaction probability $N_H \sigma_H d \sim 2 \times 10^{-3} \sigma_H^{(E)}$, obtained by using $N_H = 3.4 \times 10^{22}$ H-atoms/cm^3, with d = 600 μ.

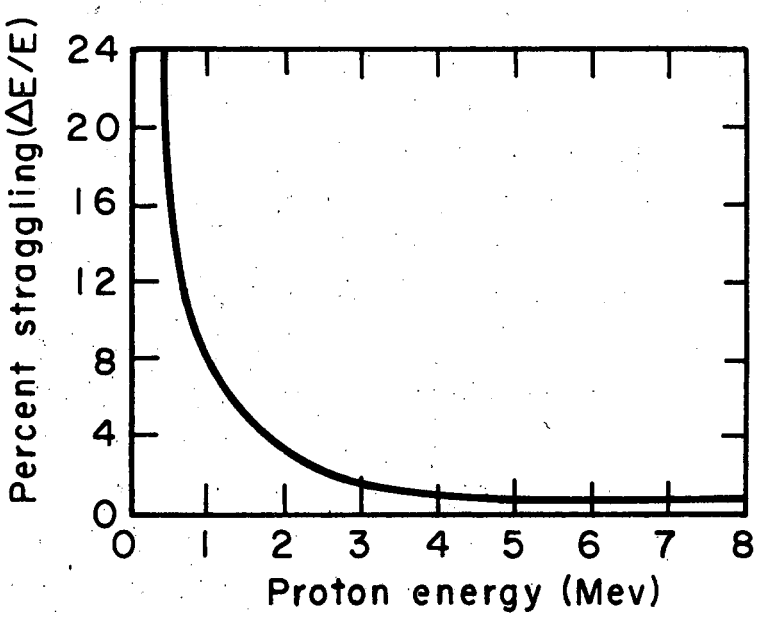

MU-22333

Fig. 15. Energy straggling of proton tracks in emulsion (after Rotblat: see Ref. 36).

Fig. 12). At neutron energies higher than 20 Mev, particles from inelastic collisions with heavy elements in the emulsion give rise to background tracks that are difficult to distinguish from valid proton tracks. Also, the $-dE/dx$ of a high-energy proton in emulsion is too small to create a track. Thus, E_{max} for Ilford E1 is limited to 20 Mev, C2 to 50 Mev, Eastman Kodak NTS to 20 Mev, and NTB to 50 Mev.

E_{min} is determined by the following factors:

(a) A minimum of 3 grains corresponding to about 2 μ is necessary for the identification of the track. For Ilford C2, this corresponds to a proton of 0.3 Mev, and for the new Ilford L2 this corresponds to 0.2 Mev.

(b) Uncertainty due to straggling increases with extreme rapidity below 0.4 Mev (see Fig. 15). Roberts predicted that by the use of special fine-grain emulsions and a careful scanning technique, the low-energy limit may be extended to 0.2 Mev.[34] For the method developed by Evans,[35] he reports that by measuring only tracks that begin or end in a 20-μ layer in the center of a 200-μ emulsion, neutron spectra up to 4.16 Mev can be measured without requiring a geometric correction factor. And by measuring only tracks that begin or end in a 100-μ layer in the center of a 400-μ and 600-μ layer respectively, and using the more elaborate development technique of Stiller et al.,[40] the method can be extended to 5.7 Mev and 7.7 Mev respectively. If the 2-mm emulsion castings of Yagoda are used, spectra can be measured up to 16 Mev. The low-energy limit is about 0.5 Mev for the method used by Evans.[35]

4. Saturation Effects

Saturation effects are determined by the readability of the recoil tracks among background track density. C2 emulsion with more than $10^9/cm^2$ and $E > 0.2$ Mev is not readable because of the high density of proton recoil tracks.

5. Gamma-Ray and Background Discrimination

Gamma rays produce no tracks in the proton sensitive emulsion, but may produce a general fog. The flux of gamma photons required to produce enough fogging to interfere with proton-track counting is about

the order of 1 at 0.1 Mev, 5 at 1 Mev, and 10 at 10 Mev. Other background effects can be discriminated visually.

6. Remarks

Advantages of the nuclear emulsion technique are its relatively high efficiency, continuous sensitivity, zero dead time, relative insensitivity to gamma and background radiation, small size, light weight, very small exposure time, and ability to store information for a relatively long period.

Its main disadvantage is the time required to count the tracks. This trouble is avoidable to a certain extent by using the method of automatic analysis of tracks suggested by Speh[37] and Barkas.[38] Other disadvantages are the problems of shrinkage and water content control, large statistical errors for a low concentration of tracks in a low flux density, and the fading of latent images.

B. Li-Loaded Nuclear Emulsion

Fast neutrons incident on a Li-loaded nuclear emulsion induce the reaction $Li^6 + n \rightarrow He^4 + H^3 + 4.63$ Mev, producing triton- and alpha-pair tracks in the emulsion. The emulsion is scanned for T- and α-pair tracks having a minimum range of 43 μ, by measuring R_α and R_T, or R_T and θ, or R_α and θ, or $R_\alpha + R_T$ and θ, to determine the neutron energy spectrum, where R_α and R_T are the ranges of the alpha and triton in emulsion respectively, and θ is the angle between them in the emulsion.

1. Efficiency

Efficiency is approximately equal to $N_{Li^6}\,\sigma_{Li^6}(E)\,d$. Using $N_{Li^6} \approx 5 \times 10^{20}$ atoms/cc and $d = 200\,\mu$. efficiency $\eta(E)$ is about $10^{-5}\,\sigma_{Li^6}(E)$. This is plotted in Fig. 16.

2. Energy Resolution

Keeping et al. obtained ΔE of approximately 0.1 for $E < 1.3$ Mev.[29]

3. Useful Neutron-Energy Range

Barton et al. made measurements in the energy range from 0.1 Mev to 2.5 Mev.[60] The presence of proton recoils having the same length as the α-T tracks makes it difficult to apply this method above 2.5 Mev. Barton et al. also state that a large resonance at 0.25 Mev and other difficulties (see remarks) render this method unreliable below 0.8 Mev.

4. Saturation Effects

Saturation effects are determined by the readability of the α-T tracks and the angle between them among background track density. The number of hydrogen atoms in the Li-loaded emulsion is about a hundred times larger than the number of Li^6 atoms, and the scattering cross section of hydrogen atoms is more than 15 times larger than the reaction cross section of Li^6 in the fast-neutron energy range. Thus,

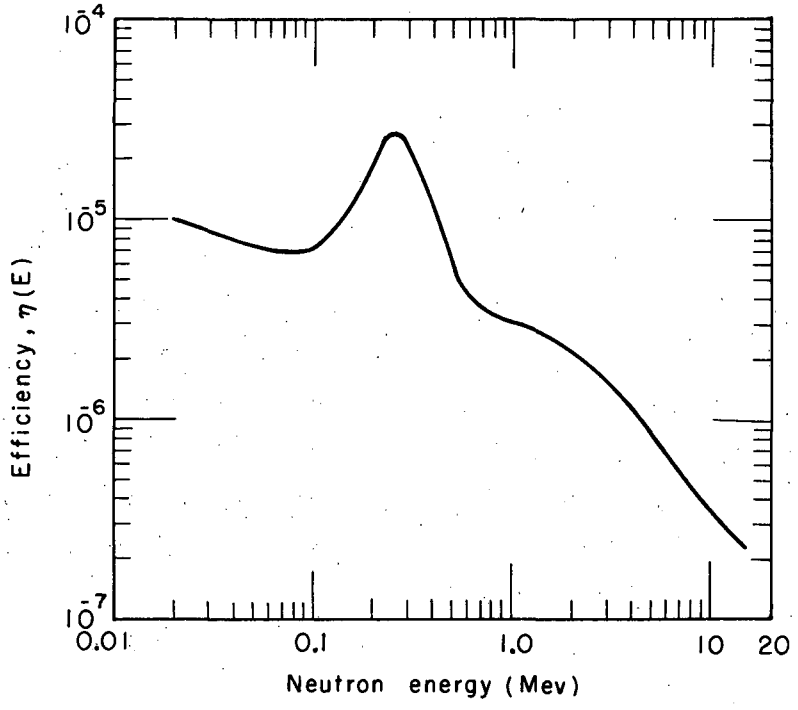

Fig. 16. Efficiency vs energy in Li-loaded emulsion, plotted from $N_{Li6}\,\sigma_{Li6}(E)d \sim 10^{-5}\sigma_{Li6}(E)$, obtained by using $N_{Li6} = 5\times10^{20}$ Li atoms per cm^3, with d = 200 μ.

saturation effects of a Li^6-loaded emulsion are essentially the same as those of the nuclear emulsion of Sec. IV-A; that is, $10^9/cm^2$, with $E > 0.1$ Mev.

5. Gamma-Ray and Background Discrimination

This effect is the same as that of the nuclear emulsion in the preceding section.

6. Remarks

Li-loaded emulsions do not need collimation and are suitable for measuring 4π neutron spectra, but the Li^6-loaded emulsion method has the following difficulties:

(a) It is hard to distinguish between α and T tracks and between α, T and proton recoil-tracks, of the same range.

(b) It is difficult to determine precisely the point of origin of tracks. However, Roberts et al. removed this difficulty by loading Li^6 into an emulsion in the form of glass beads,[42] so that the origin of α-T events in the glass bead could be easily seen in the microscope.

(c) The differential cross section for the reaction as a function of neutron energy is not well known.

(d) There is a large resonance at 0.25 Mev which complicates interpretation.

(e) Rotblat and Tai studied the shrinkage of a Li^6-impregnated emulsion and estimated an error in track length of the order of 50% for nearly vertical tracks.[41]

V. THRESHOLD DETECTORS AS 4π NEUTRON SPECTROMETERS

A series of threshold detectors having different thresholds can be employed to obtain a crude measurement of the energy spectrum of the neutron flux. The value of average-reaction cross section is obtained by measuring the radioactivity induced in the detector by a known flux with the same distribution of neutron energies as the flux to be measured. At best, threshold detectors do not give a very accurate determination of the energy spectrum of the neutron flux, but when accuracy is not too important this method has the advantage of simplicity.

1. Efficiency

The efficiency of threshold detectors depends upon the reaction cross section $\sigma(E)$ of the various activated materials used. Cowan and O'Brien obtained a greatly improved efficiency, compared with the conventional instrument, by using scintillation detectors in which activated materials are an integral part of the scintillator.[43]

The table compiled by Cowan and O'Brien is inserted here for comparison.

Table I. Comparison of Various Threshold Detectors

Reaction Used	Threshold (Mev)	Min. detectable Neutron flux ($n/cm^2/sec$)	Efficiency %	Half-life
$U^{238}(n.f)$	1.1	6.6	10^{-3}	---
$P^{31}(n.p)Si^{31}$	2.0	200	---	160 min
$S^{32}(n.p)P^{32}$	2.0	230	5	14.5 d
$Ag^{107}(n.2n)Ag^{106}$	9.6	350	8-10	24.5 min
$I^{127}(n.2n)I^{126}$	10	20	---	13 d
$C^{12}(n.2n)C^{11}$	20	2.3	90	20.3 min

2. Energy Resolution

Threshold detectors do not give accurate measurement of the neutron-energy spectrum and are used only when a crude determination of the energy spectrum is required.

3. Saturation Effects

By adjusting irradiation time, cooling time, and counting time, there is practically no upper limit to the maximum neutron flux that can be counted. The actual minimum detectable neutron flux is five to ten times the value given in Table I, before reasonably accurate measurement can be made. By irradiating and counting for a longer time, fluxes of the order of 1 n/cm^2 per sec can be detected, and measurements can be made in the region of 5 to 10 n/cm^2 per sec.[43]

4. Gamma and Background Response

Gamma-ray and background response varies with threshold detectors. Most threshold detectors have interfering reactions and must therefore be used with care. Such materials as Al and Mg are used for counter construction in order to minimize spurious background from gamma-induced fission.

5. General Remarks

The foils used as threshold detectors are usually too insensitive. A great improvement in sensitivity can be obtained by the use of a scintillation technique instead. However, threshold detectors are well suited for use where a reaction is extremely short, such as radiation bursts from critical assemblies or nuclear explosions.

VI. SEMICONDUCTOR FAST-NEUTRON DETECTOR

A charged particle passing through a semiconductor creates electron-hole pairs. If created in the depletion zone of a p-n junction, or in a surface barrier where an appreciable field exists, these carriers may be separated by the field. This produces a pulse which can be amplified and counted. The resultant pulse-height spectrum is differentiated, and then unfolded when necessary, to obtain the neutron energy spectrum. In order to detect fast neutrons, they must react with some outside nucleide to produce charged particles, such as p, α, and fission products, which can be detected. Some nucleides that may be used are: hydrogenous materials for recoil of protons; Th^{232}, U^{238}, Np^{237} for fast fission products; $N^{14}(n,p)\,C^{14}$, $S^{32}(n,p)\,P^{32}$ for protons, and $Li^{6}(n,\alpha)H^{3}$, or $B^{10}(n,\alpha)\,Li^{7}$ with paraffin cover for α particles.

1. Efficiency

The efficiency of a semiconductor depends upon the reaction probability of the material we use to get charged particles. Higher efficiency is obtained by using thicker material, but the thickness should be small compared with the minimum range of charged particles produced inside the material, so that a sharp energy resolution may be obtained. For example, the range of a 1-Mev α particle within $Li^{6}F$ is about 3μ. Using 0.5-μ thick $Li^{6}F$, we get a reaction probability of about 10^{-6}. Thicker reacting material can be used at higher-neutron energy, but the reaction cross section usually decreases for higher-energy neutrons and vice versa for lower-energy neutrons. Thus the efficiency of a semiconductor using $Li^{6}F$ is of the order of 10^{-6} in the fast-neutron energy range. Thus the counting rate of a semiconductor is rather low because of its small size and low efficiency. The counting rate can be increased by using larger areas combined with deeper depletion layers, or by stacking 5 or 10 semiconductors together. Efficiency increases as energy increases at high energies when a thick paraffin layer with Li^{6}

or B^{10} is used as an activator.

Love and Murray obtained an efficiency of approx 10^{-6} for 2-Mev neutrons, using 150-$\mu g/cm^2$-thick Li^6F layers evaporated onto a Si-Au surface-barrier counter.[44]

2. Energy Resolution

Energy resolution appears limited by the noise level of the amplifier and the thickness of activation material used. It requires only about 3 ev to produce an electron-hole pair in a semiconductor, as compared to about 30 ev for an ion pair in a gas. Thus, for the same amount of the energy deposited in the sensitive volume of each detector, the standard deviation of a semiconductor is reduced by a factor of approx $10^{-1/2}$. Therefore, energy resolution of semiconductor is extremely high.

Barshal et al. obtained 0.6% resolution at 6 Mev for an α particle,[45] and Love and Murray obtained ΔE approx 0.3 Mev for energies between 0.6 and 3.5 Mev.[44] Dearnaley et al. obtained an energy resolution of 1.3% at room temperature with a 15 mm^2 Au-Si detector.[46] Most impressive of all, Dearnaley reports that 0.38% resolution has been obtained for 5.48-Mev α particles at 77° K. Use of a low-noise cascade preamplifier, and reduction of stray capacitance to a minimum, should result in even better energy resolution.

3. Useful Energy Range

Friedland reports a linear response to protons up to 4.5 Mev and to α particles up to at least 20 Mev, obtainable with a suitable reverse bias.[47] Dearnaley et al. predict that a linear response to protons up to 10 Mev may be achieved.[46] By using a suitable activation material with the width of the depletion layer of a suitable semiconductor greater than the distance necessary to dissipate most of the energy of charged particle from maximum neutron energy we want to count, we should be able to detect any fast neutrons below 20 Mev.

4. Gamma-Ray and Background Discrimination

Gamma rays may deposit only a very small amount of their energy in the sensitive region due to its small size, and by appropriate pulse-height biasing we can obtain a semiconductor relatively insensitive to both gamma rays and background radiation, except for pileup phenomena encountered in an extremely high flux.

On radiation damage in semiconductors, Babcock et al. report that an exposure corresponding to 5×10^{9} fission fragments per cm^{2} produced no change in counting efficiency.[48]

5. Time Response

Dearnaley and Whitehead report that a pulse-rise time of less than 3×10^{-9} sec has been measured. They calculated that rise time should be about 5×10^{-10} sec at 77^{o} K.[46]

6. Directionality

The semiconductors using such reactions as $Th^{232}(n, f)$, $U^{238}(n, f)$, $Np^{237}(n, f)$, $N^{14}(n, p)C^{14}$, and $S^{32}(n, p)P^{32}$ to get charged particles are nondirectional, while those semiconductors that use hydrogenous materials for recoil protons, or Li^{6}, B^{10} with a paraffin cover for α particles, are directional.

7. Remarks

Dearnaley et al.[46] think a p-i-n detector should extend the range of usefulness considerably. N. A. Bailey, of Hughes Aircraft in Los Angeles, claims that he has made a detector of Li drifted into Si with a sensitive layer about 3-mm thick that can accomodate protons up to more than 20 Mev with an energy resolution of 3%.

The semiconductor neutron spectrometer, due to its extremely good energy resolution, fast time response, insensitively to gamma rays, small size and broad fast-neutron energy range, promises to replace the scintillation counter as most used for the wide variety of purposes after further development.

VII. CONCLUSIONS

In general, no particular counter can satisfy all the requirements for different situations. Table II and Figs 17 and 18 were constructed so that they might be useful in selecting a desired counter for a different situation. However, for the case where a high counting rate is not required, further development of semiconductor neutron spectrometers seems most promising because of their extremely high energy resolution, fast time response, broad neutron-energy range, insensitivity to gamma rays and small size. It seems these will replace the scintillation counter as the most used for a wide variety of purposes after further development. The counting rate of semiconductors can be improved by various methods stated in Sec. VI, but it seems it will not have the high efficiency possessed by such a counter as the plastic scintillator.

Where high energy resolution is not required and where high efficiency is required, further development of a plastic scintillator in which it is possible to discriminate gamma rays using the methods suggested in Sec. II-**A**, and a development of methods to differentiate and unfold pulses to get the neutron spectrum without introducing large errors, is required.

Table II. Comparison of 4π Fast-Neutron Spectrometers

	Instrument	Typical Efficiency	Typical Energy Resolution (%)	Useful Neutron Energy Range (Mev)	Decay Time in sec, or Saturation Effects	Gamma Sensitivity	Reactions	Advantages	Disadvantages	References
Scintillation Counters	Plastic	See Fig. 1	See Fig. 2	0.1-20	3 mμ-4.6 mμsec	Sensitive	Proton recoil	High efficiency, fast decay time	High gamma sensitivity	[8], [9], [3], [10], [12], [5], [7], [1], [11], [2], [6],
	He^4	See Fig. 3	<10% above 5 Mev ~10% at 5 Mev >10% below 5 Mev	0.1-20	~1 mμsec	Insensitive	Alpha recoil	Insensitive to γ rays, fast decay time	Low efficiency	[15], [14], [26], [57], [13], [54], [45]
	$Li^6I(Eu)$	See Fig. 4	See Fig. 5	1-14	1.2 μsec	Biasable due to 4.78 Mev Q-value	$Li^6+n \rightarrow He^4+T+4.78$ Mev	High efficiency	Cool to liquid nitrogen point for improved resolution	[17], [53]
	Cd-Loaded Organic Liquid	~85% for 30X30 in.	~10% at 1 Mev ~40% at 10 Mev	1-20	~1 mμsec	Good discrimination due to delayed coincidence and 9.2 Mev Q-value	$Cd^{113}+n \rightarrow Cd^{114}+\gamma+9.2$ Mev	High efficiency, good for low counting exp; easy γ biasing	Poor energy resolution	[19], [20], [18]
Proportional Counters	$He^3(n,p)T$	See Fig. 8	~50% 0.1 Mev ~10% 1 Mev ~ 5% 10 Mev	0.1-1.025	~1 μsec	Biasable due to 0.77 Mev Q-value	$He^3+n \rightarrow p+T+0.77$ and He^3 recoil	Easy γ biasing, High efficiency	Low efficiency narrow useful energy range	[23], [56], [24], [50], [51], [27], [26], [57], [16],
	Paraffin-Moderated BF_3	$\sim 10^{-2}$ See Fig. 10	~50% - 100%	0.01-10	~1 μsec	Biasable due to 2.78 Mev Q-value	$B^{10}+n \rightarrow d+Li^7+2.78$ Mev	High energy resolution, easy γ biasing	Poor energy resolution	[28], [11]
	Polyethylene-Lined	See Fig. 11	Measure energy flux	0.2-20	~1 μsec	Insensitive	Proton recoil	Insensitive to γ rays	Low efficiency, cannot measure energy spectrum	[30], [31]
Photographic Methods	Nuclear Emulsion	See Fig. 14	~10-100%	0.2-20	$\sim 10^9$ n/cm² E > 0.1	~1 r of 0.1 Mev ~5 r of 1 Mev ~10 r of 10 Mev (gammas permissible)	Proton recoil	High efficiency, no dead time, insensitive to γ rays, small size, small exposure time	Large amount of time required to measure tracks, shrinkage control	[32], [33], [34], [35], [36], [37], [38], [49], [55]
	Li-Loaded Emulsion	See Fig. 16	ΔE ≈ 0.1 Mev for E < 1.3 Mev	0.1-16	~109 n/cm² E > 0.1	Same as above (nuclear emulsion)	$Li^9+n \rightarrow He^4+H^3+4.78$ Mev	Same as above	Same as above; low efficiency	[35], [39], [40], [41], [42], [60]
Threshold Detectors		See Table I	~50-100%	0.01-20	No Saturation	Sensitive	$U^{238}(n,f)$ $P^{31}(n,p)Si^{31}$ $S^{32}(n,p)P^{32}$ $Ag^{107}(n,2n)Ag^{106}$	Extremely short reaction time, simple to use	Poor energy resolution, high background effect	[43]
Semiconductors		$\sim 10^{-5}$-10^{-7}	Extremely high, up to 0.2%	0.01-20	~10-0.1 mμsec	Insensitive	$Th^{232}(n,f)$ $N^{14}(n,p)C_{14}$ $Li^6(n,\alpha)H^3$ Proton recoil	Extremely good energy resolution, extremely fast decay time, insensitive to γ rays, small size, broad energy range	Low counting rate	[45], [44], [46], [47], [48], [52]

NOTE: The 20 Mev and 0.01 Mev, as the E_{max} and E_{min} quoted above, imply just E_{max} and E_{min} of fast-neutron energy ranges we are interested in, and do not imply the counter cannot be used at higher or lower than 20 Mev and 0.01 Mev.

Figure 17. Efficiency vs energy of various counters at the conditions stated for comparison: The relative vertical positions of curves are not fixed but can be moved up or down vertically by several factors, by changing the conditions stated. The top curve does not imply the best counter. It merely states that it has a relatively high efficiency. The usefulness of a counter is determined by various factors such as energy resolution, gamma sensitivity, energy range and time response as well as by efficiency.

Curves (1)(2)(3)(5)(8)(9)(11) are drawn from the calculated reaction probabilities and represent the highest theoretically possible efficiency at the conditions stated. Downward arrows are drawn to indicate that the actual efficiency will be smaller by several factors. Curve (4) is the probable range of efficiency for a large (~ 30 in. × 30 in.) Cd-loaded organic scintillator. Curve (6) shows an efficiency of the order of 10^{-2} in the energy range shown. Curve (1) is the calculated efficiency of Moyer (Ref. 30). Curve (10) shows the threshold energy of various threshold detectors of Cowan and O'Brien (Ref. 43) with the order of their efficiency.

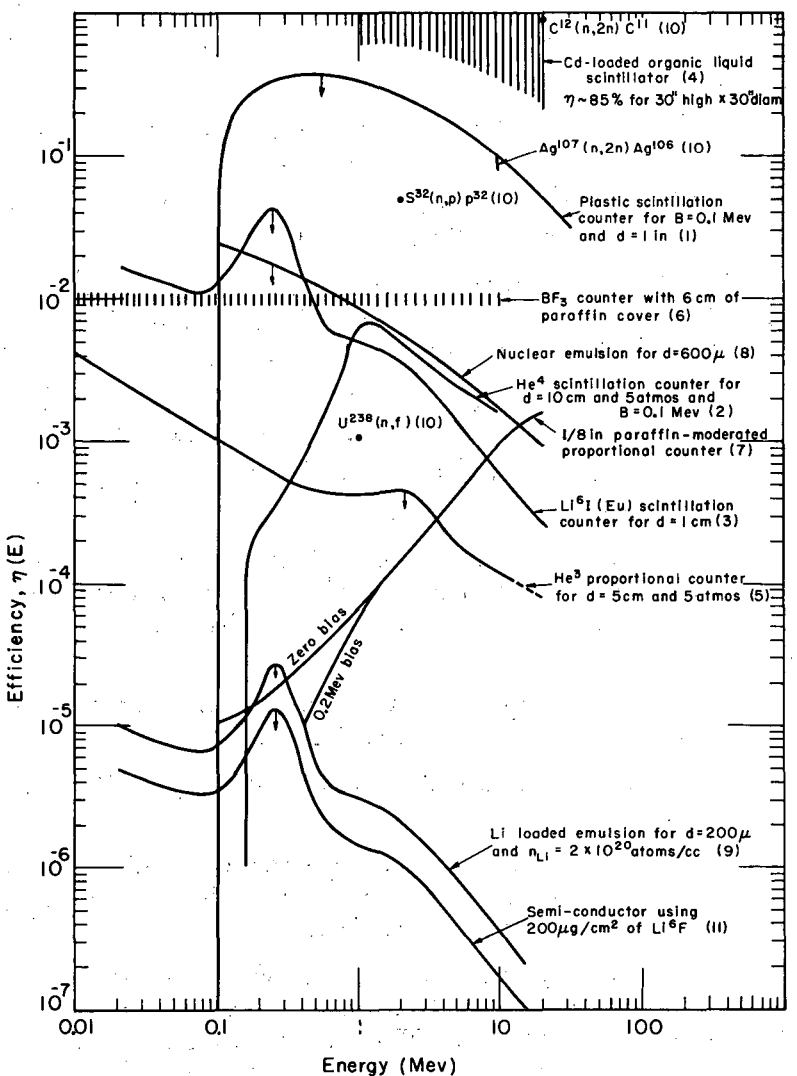
$C^{12}(n,2n)C^{11}$ (10)
Cd-loaded organic liquid scintillator (4)
$\eta \sim 85\%$ for 30" high x 30" diam
$Ag^{107}(n,2n)Ag^{106}$ (10)
$S^{32}(n,p)P^{32}$ (10)
Plastic scintillation counter for B = 0.1 Mev and d = 1 in (1)
BF_3 counter with 6 cm of paraffin cover (6)
Nuclear emulsion for d = 600 μ (8)
He^4 scintillation counter for d = 10 cm and 5 atmos and B = 0.1 Mev (2)
$U^{238}(n,f)$ (10)
1/8 in paraffin-moderated proportional counter (7)
Li^6I (Eu) scintillation counter for d = 1 cm (3)
He^3 proportional counter for d = 5 cm and 5 atmos (5)
Zero bias
0.2 Mev bias
Li loaded emulsion for d = 200 μ and $n_{Li} = 2 \times 10^{20}$ atoms/cc (9)
Semi-conductor using 200 μg/cm² of Li^6F (11)
Efficiency, η(E)
10^{-1}
10^{-2}
10^{-3}
10^{-4}
10^{-5}
10^{-6}
10^{-7}
0.01
0.1
1
10
100
Energy (Mev)

MU-23272

Figure 18. Qualitative relation between efficiency and energy resolution for various counters.

(1) Plastic scintillation counter for d=1 inch and B=0.1 Mev. Drawn from Figs. 1 and 2.

(2) He^4 scintillation counter for d=10 cm and 5 atmos., and B=0.1 Mev. Drawn from Fig. 3 and the energy resolution obtained by Eggler and Huddleston i.e., 10% at 5 Mev (see Ref. 14).

(3) $Li^6I(Eu)$ scintillation counter for d=1 cm.

(4) Cd-loaded liquid scintillator. Drawn from the estimates made in Sec. II-D.

(5) He^3 proportional counter for 5 atmos. and d=5 cm. Drawn from Fig. 8 and the energy resolution obtained by Batchelor et al., i.e., about 5% at 0.12 Mev and 12% at 1 Mev (see Ref. 23).

(6) BF_3 counter with 6 cm of paraffin cover. Drawn from the estimates made in Sec. III-B.

(8) Nuclear emulsion for d=600 μ. Drawn from Fig. 14 and $\Delta E \simeq 1$ Mev.

(9) Li^6-loaded emulsion for d=200 μ and $N_{Li} = 5 \times 10^{20}$ atoms/cc. Drawn from Fig. 16 and $\Delta E \simeq 0.1$ Mev for $E < 1.3$ Mev as obtained by Keepin et al. (see Ref. 39).

(11) Semiconductors. Drawn from the best energy resolution of 0.38% obtained by Dearnaley et al. (Ref. 46) and the efficiency range of 10^{-5} - 10^{-7}. The sideward arrow is drawn to indicate that usually a poorer energy resolution than the indicated value is obtained.

Downward arrows are drawn to indicate that the actual efficiency will be smaller by several factors. Numbers on curves indicate neutron energy in Mev.

The range of efficiency (η) of various counters is of the order of the seventh power, while the range of energy resolution (δ) of these counters is of the order of the third power. The η/δ vs energy does not give correct intepretation of the importance of the counter, since the small variation in the range of energy resolution is more important than the same variation in the range of efficiency.

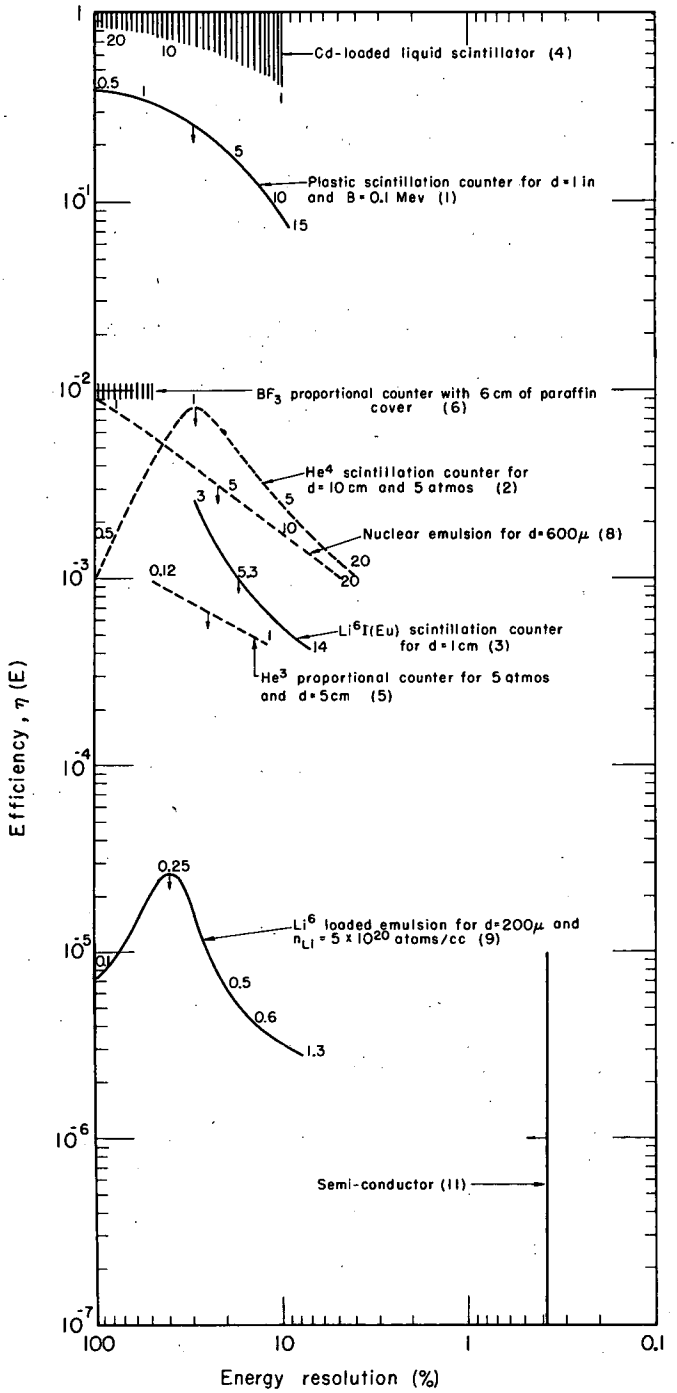
Cd-loaded liquid scintillator (4)
Plastic scintillation counter for d = 1 in and B = 0.1 Mev (1)
BF3 proportional counter with 6 cm of paraffin cover (6)
He4 scintillation counter for d = 10 cm and 5 atmos (2)
Nuclear emulsion for d = 600μ (8)
Li6I(Eu) scintillation counter for d = 1 cm (3)
He3 proportional counter for 5 atmos and d = 5 cm (5)
Li6 loaded emulsion for d = 200μ and nLi = 5 x 10^20 atoms/cc (9)
Semi-conductor (11)
Efficiency, η (E)
Energy resolution (%)
MUB-638

ACKNOWLEDGMENTS

This work was conducted under the guidance of Dr. Roger W. Wallace of the Lawrence Radiation Laboratory at Berkeley, and the author would like to thank him for his support, encouragement and advice throughout.

This work was done partly under the auspices of the U. S. Atomic Energy Commission, and partly under U. S. Air Force contract AF 29(601)-2784.

REFERENCES

1. C. D. Swaltz and G. E. Owen, in Fast Neutron Physics, Part I, ed. by J. B. Marion and J. L. Fowler, (Interscience Publishers, Inc., New York, 1960), Chap. 2B.
2. B. V. Rybakov and V. A. Sidorov, Fast Neutron Spectroscopy, trans. from the Russian by Consultant's Bureau, Inc., New York, 1959.
3. G. F. J. Garlick and G. T. Wright, Proc. Phys. Soc. (London) 65B, 415 (1952).
4. J. B. Birks, Phys. Rev. 95, 277 (1954).
5. C. O. Muelhause, in Fast Neutron Physics, Part I, (Interscience Publishers, Inc., New York, 1960), Chap. 2B.
6. R. K. Swank, Ann. Rev. Nuclear Sci. 4, 111 (1954).
7. R. B. Owen, Nucleonics, 17, 92 (1959).
8. F. D. Brooks, Nuclear Inst. of Methods 4, 151 (1959).
9. B. Brown and E. B. Hooper, Jr., Nucleonics 16, 96 (1958).
10. J. H. McCrary, H. L. Taylor, and T. W. Bonner, Phys. Rev. 94, 808 (1954).
11. H. A. Taylor, O. Lonsjo, and T. W. Bonner, Phys. Rev. 100, 174 (1955).
12. W. G. Moulton and C. W. Sherwin, Rev. Sci. Instr. 20, 366 (1949).
13. J. A. Northrup and R. A. Nobles, Nucleonics 14, 36 (1956).
14. C. Eggler and C. M. Huddleston, Nucleonics 14, 34 (1956).
15. R. W. Diekieson, A Noble Gas Scintillation Counter (M.S. Thesis), University of California Radiation Laboratory Report UCRL-3794, May 28, 1957 (unpublished).
16. D. West, Energy Measurements with Proportional Counters, in Progress In Nuclear Physics, Vol. 3 (Pergamon Press, Ltd., London, 1953), p. 18.
17. R. B. Murray, Nuclear Instr. 2, 237 (1958).

18. F. Reines, C. L. Cowan, Jr., F. B. Harrison, and D. S. Carter, Rev. Sci. Instr. 25, 1861 (1954).
19. P. T. Andrews, Rev. Sci. Instr. 28, 56 (1957).
20. C. O. Neuhlhause, Nucleonics 14, 38 (1956).
21. L. J. Nicastro and R. S. Caswell, A Double-Pulse Total-Absorption Fast-Neutron Spectrometer, NBS Technical Note No. 1, Washington, D. C., 1959.
22. L. E. Beghian, R. A. Allen, J. M. Calvert, and H. Halban, Phys. Rev. 86, 1044 (1952).
23. R. Batchelor, R. Aurs, and T. H. R. Skyrme, Rev. Sci. Instr. 26, 1037 (1955).
24. A. L. Cockcroft and S. C. Curran, Rev. Sci. Instr. 22, 37 (1951).
25. B. B. Rossi and H. H. Staub, Ionization Chambers and Counters: Experimental Techniques (McGraw-Hill Book Company, Inc., New York, 1949).
26. G. Salvini, Rev. Sci. Instr. 19, 494 (1958).
27. C. M. Huddleston, Gaseous Scintillation Detectors, in Proceedings of the Second United Nations International Conference on the Peaceful Uses of Atomic Energy, Vol. 14 (United Nations, Geneva, 1958), p. 688.
28. W. N. Hess, W. W. Patterson, R. Wallace, and E. L. Chupp, Phys. Rev. 116, 445 (1959).
29. R. Wallace, B. J. Moyer, W. W. Patterson, A. R. Smith, and L. D. Stephens, The Dosimetry of High-Energy Neutrons Produced by 0.2 Mev Protons Accelerated in the Bevatron, Lawrence Radiation Laboratory Report UCRL-~~9412~~ 9214, 1960 (unpublished).
30. B. J. Moyer, Nucleonics 10, 14 (1952).
31. B. W. Thompson, Fast-Neutron Scintillation Survey Meter, University of California Radiation Laboratory Report UCRL-2357, October 28, 1953 (unpublished).
32. F. Reines, Phys. Rev. 74, 1565-L (1948).
33. M. Nereson and F. Reines, Los Alamos Scientific Laboratory Report LA-1190, 1950 (unpublished).

34. J. H. Roberts, Rev. Sci. Instr. 28, 677 (1957).
35. J. E. Evans, The Two-Plate Method of Measuring Fast Neutron Energy Spectra When the Direction of the Incident Neutrons cannot be Determined, Los Alamos Scientific Laboratory Report LAMS-1312, 1951 (unpublished).
36. J. Rotblat, Photographic Emulsion Technique, in Progress in Nuclear Physics, Vol. 1 (Pergamon Press, Ltd., London, 1950).
37. K. C. Speh, Atomatic Analysis of Tracks in Nuclear Emulsion, in Proceedings of the Second United Nations International Conference on the Peaceful Uses of Atomic Energy, Vol. 14 (United Nations, Geneva, 1958), p. 372.
38. W. H. Barkas, Equipment and Method of Automatic Track Analysis, Lawrence Radiation Laboratory Report UCRL-8482, Aug. 14, 1958. (unpublished).
39. G. R. Keepin and J. H. Roberts, Rev. Sci. Instr. 21, 163 (1950).
40. B. Stiller, M. Shapiro, and F. O'Dell, Bull. Am. Phys. Soc. 26, 16 (1951).
41. J. Rotblat and C. T. Tai, Nature A168, 835 (1949).
42. J. H. Roberts and F. E. Kinney, Rev. Sci. Instr. 28, 610 (1957).
43. F. P. Cowan and J. F. O'Brien, Methods of Measurements of Neutron Flux at Low Levels, in Proceedings of the International Conference on the Peaceful Uses of Atomic Energy, Geneva, 1955, Vol. 14 (United Nations, New York, 1956).
44. T. A. Love and R. B. Murray, Use of Silicon Surface Barrier Counter in Fast Neutron Detection and Spectroscopy, Oak Ridge National Laboratory Report ORNL Central File No. 60-5-121, May 31, 1960, (unpublished).
45. H. H. Barschall, R. F. Taschek, L. Rosen, and J. H. Williams, Rev. Mod. Phys. 24, 1 (1952).
46. G. Dearnaley and A. B. Whitehead, Surface-Barrier-Charged Particle Detectors, Atomic Energy Research Establishment Report AERE-R3278, Harwell, Berks, England, 1960 (unpublished).
47. S. S. Friedland, J.W. Mayer, and J.S. Wiggins, Nucleonics 18, 54 (1960).

48. R. V. Babcock, R. E. Davis, S. L. Ruby, K. H. Sun, and E. D. Wooley, Nucleonics 17, 116 (1959).
49. A. Beiser, Rev. Mod. Phys. 24, 273 (1952).
50. N. P. Glazkov, An He^3-Camera for Neutron Spectroscopy, Instr. and Exptl. Tech. (USSR) 4, 96 (1957).
51. J. N. Green, Preliminary Testing of a Proportional Counter for Neutron Spectroscopy with He^3 (M.S. Thesis) University of California Radiation Laboratory Report UCRL-8274, April 21, 1958 (unpublished).
52. K. G. McKay and K. B. McAffee, Phys. Rev. 91, 1079 (1953).
53. T. R. Ophel, Nuclear Instr. 3, 45 (1958).
54. J. R. Pickens, Work with a Noble-Gas Scintillation Counter, Lawrence Radiation Laboratory Report UCRL-8295, 1958 (unpublished).
55. L. Rosen, Nucleonics 11, 32 and 38 (1953).
56. R. Batchelor and G. L. Morrison, in Fast Neutron Physics, Part I, (Interscience Publishers, Inc., New York, 1960), Chap. 3C.
57. J. A. Northrop, J. L. Gursky, and A. E. Johnrud, Further Work with Noble-Element Scintillators, 6th Scintillation Counter Symposium, Washington D. C., January 27, 1958.
58. A. Sayres and C. S. Wu, Rev. Sci. Instr. 28, 758 (1957).
59. W. Bothe and V. W. Stetter, Naturforsch. 6A, 61 (1951).
60. D. M. Barton et al., The Li^6 Photographic Plate Method of Measuring Neutron Spectra, Los Alamos Scientific Report LA-1526, 1952 (unpublished).